ISSN 0280–5316
ISRN LUTFD2/TFRT--5576--SE

# Manual Control of Unstable Systems

Sabina Brufani

Department of Automatic Control
Lund Institute of Technology
February 1997

**Department of Automatic Control**
**Lund Institute of Technology**
**Box 118**
**S-221 00 Lund Sweden**

*Document name*
Master Thesis

*Date of issue*
February 1997

*Document Number*
ISRN LUTFD2/TFRT--5576--SE

*Author(s)*
Sabina Brufani

*Supervisor*
Karl Johan Åström

*Sponsoring organisation*

*Title and subtitle*
Manual Control of Unstable Systems. (Manuell reglering av instabila system).

*Abstract*

Automatic control is increasingly used in mission critical applications. The reason for this is the potential benefits and the fact that control engineering is now able to deal with complex systems. Control of high performance aircrafts is a typical example. Considerable benefits can be obtained by having an aircraft that is unstable in certain flight conditions and providing stability with a control system. The unstable flight conditions typically include the low speed conditions that occur during take off and landing. The aircrafts have hydraulic actuators that saturate for large signals or signal rates. Since the feedback loop is broken in saturation the unstable states may diverge to situations which cannot be recovered. The presence of a pilot is yet another complication because the pilot may also drive the system unstable through manual control actions. Design of control systems for such situations is a significant challenge. Aircraft manufacturers have encountered severe difficulties because of this problem which has led to severe delays of projects. The design of control laws for unstable systems that make it impossible for the pilot to drive the system unstable while maintaining good handling qualities is a challenging problem. The goal of this thesis is to develop insight into this problem. A strongly simplified case that captures the key elements of the problem is first solved to get some insight. This shows that it is possible to developed a hybrid strategy which has interesting problems. A more realistic problem is simultaneous stabilization and control of the pivot of an inverted pendulum. This problem is nice because it also allows easy verification in the laboratory. The problem is investigated and control strategies are designed by combining several different strategies using the hybrid approach. The properties of the strategies are illustrated by simulation. Finally we make a preliminary attempt at applying the ideas to the flight control problem. The conclusion of the work is that the approach taken appears promising and worthy of further studies.

*Key words*

*Classification system and/or index terms (if any)*

*Supplementary bibliographical information*

*ISSN and key title*
0280–5316

*ISBN*

*Language*
English

*Number of pages*
53

*Recipient's notes*

*Security classification*

# Contents

# 1. Introduction

This thesis deals with problems that occur in manual control of unstable systems with saturating actuators. Such a system can always be driven unstable with disturbances that are sufficient large. The system runs open loop when the actuator saturates. The unstable state will then diverge. If this state is sufficiently large it is impossible to recover with the limited control actions. To control the systems manually it is necessary to provide them with a stabilizing feedback. It is then interesting to find out if the manual control actions may drive the system unstable, or if it is possible to find a control system which maintains stability and admits manual control. These problems are fundamental when dealing with dangerous systems where loss of stability has dramatic consequences. The key task is to assure that no manual input will drive the system to a configuration from where the limited control actions are unable to recover it.

As the stability of the system is increased the maneuverability is decreased. The idea used in this thesis is to give priority to manual control when the condition of the system are safe, and decrease the maneuverability as the region where controllability is lost is approached. This is achieved with an hybrid strategy. First several independent control strategies are designed, then they are patched together so that more authority is given to one or to another one depending which region the system is. A key problem is the shaping of the regions where the different strategies act. The results that are achieved in this way give good results from simulations. The problem that arises when dealing with hybrid controllers is that is very difficult to investigate on the behavior of the system. Particular attention must be payed to the way of mixing controllers, and the switching from one to the another. The problem of saturations of actuators in unstable dangerous system appear in the control of high performance military aircrafts. A typical example is the JAS 39 Gripen. In this case the essential limitations are due to rate saturations in the hydraulics. In the JAS program much effort was devoted to the allocation of control authority between manual control and stabilization Rundqwist (1996). The multivariable nature of the problem gave rise to additional difficulties. In this thesis we will investigate the problem of level saturation which is a little simpler. We will also restrict ourselves to single input systems.

In chapter 2 the control of a simple unstable system is effectued with a hybrid strategy. The simplicity of the problem make it possible to capture the main features of the hybrid strategy. . It turns out that many of the fundamental problems can be discussed using this example. In chapter 3 the strategy is applied to the control of a classical unstable non linear system: the inverted pendulum. This problem is nice because it also allows easy verification in the laboratory. The problem is investigated and control strategies are designed by combining several different strategies using the hybrid approach. Flight dynamics is discussed in Chapter 4.

This chapter gives the basic equations for flight dynamics. The mechanisms that lead to instability are also investigated. In Chapter 5 we make a preliminary attempt at applying the ideas to the flight control problem.

# 2. Mixing control strategies

When controlling unstable system such us inverted pendulum we have a number of conflicting goals to be reached. To obtain a control strategy that will allow the manual control of the inverted pendulum and at the same time will stabilize it we will mix different control laws.
The concept that will lead the way of mixing the strategies is that priority must always be given to the stability of the system. Is complicate to understand how the pendulum controlled by the hybrid strategy behaves. To capture the fundamental issues of the hybrid strategy we will apply it to a simpler system. The system that we will analyze is a second order linear unstable system.

## 2.1 A simplified problem

Consider the system

$$\begin{aligned} \frac{dx_1}{dt} &= x_1 - u \\ \frac{dx_2}{dt} &= u \\ |u| &\leq u_m \end{aligned}$$

The porpoise of the control is to stabilize the state $x_1$ at the equilibrium point $x_1 = 0$, and to permit the manual control of the variable $x_2$. We will also assume that the control variable is limited $|u| \leq u_m$.

### Control design

We will now design control strategies for the problem. For simplicity we will only consider two strategies:
-A stabilizing strategy
-A strategy for controlling the variable $x_2$.
These strategies will be designed based on linear theory.

### The stabilizing strategy

In this strategy we will focus on the first equation. We will simply design a strategy that stabilize $x_1$. This can be accomplished by:

$$u_s = k_s x_1 \tag{2.1}$$

The closed loop system becomes

$$\frac{dx_1}{dt} + (k_s - 1)x_1 = 0$$

To obtain a stable system we must choose $k_s > 1$.

### A stabilizing strategy that admit the control of $x_2$

Now we will derive a control strategy that stabilizes the first state and admits set point control of the second state. This can be accomplished with:

$$u_c = l_1 x_1 + l_2(x_2 - r) \tag{2.2}$$

where $r$ is the command signal. Introducing this control strategy into equations (2.2) and making the Laplace transform we get:

$$\begin{aligned}(s - 1 + l_1)X_1(s) + l_2 X_2(s) &= l_2 R \\ -l_1 X_1(s) + (s - l_2)X_2(s) &= l_2 R\end{aligned}$$

Elimination of $X_1(s)$ gives:

$$X_2(2) = \frac{l_2(s-1)}{s^2 + s(l_1 - l_2 - 1) + l_2} R$$

Choosing a design that gives the closed loop characteristic polynomial:

$$s^2 + 2\omega\zeta s + \omega^2 = 0$$

we get

$$\begin{aligned}l_1 &= \omega^2 + 2\omega\zeta + 1 \\ l_2 &= \omega^2\end{aligned}$$

### Combining the strategies

The question is now how the control strategies (2.2) and (2.1) should be combined.It is intuitively clear that highest priority must be given to the stabilizing strategy (2.1). If there is a danger that the system becomes unstable all effort should be concentrated on stabilization. This is of course particularly critical if the state variable $x_1$ approaches $|x_1| = u_m$, because the system will be lost if $|x_1| > u_m$. The state variable $x_1$ will then diverge no matter what control actions are taken.
One possibility is to arrange a system as follows:

Where $v$ and $u_s$ have the following expression:

$$\begin{aligned}v &= (l_1 - k_s)x_1 + l_2(x_2 - r) \\ u_s &= k_s x_1\end{aligned}$$

The control signal from the outer loop is limited to

$$-v_m \leq v \leq v_m$$

where $v_m$ represents the control authority assigned to the regulation task. As a result of the hybrid strategy represented by figure 2.1 five different

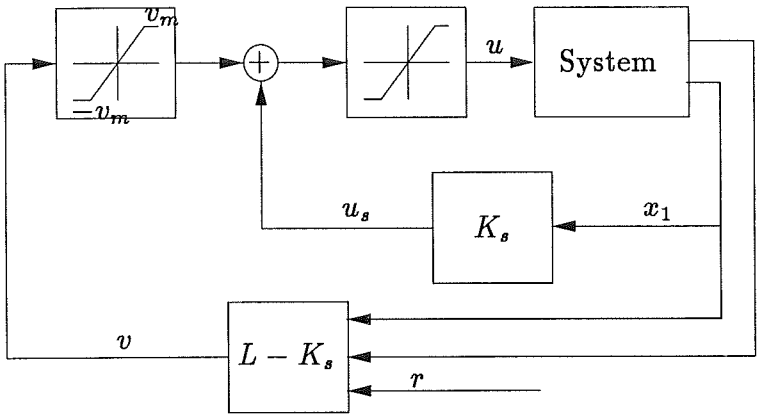


**Figure 2.1** An hybrid strategy

regions can be identified in the plane $x_1$, $x_2$. In each region a different linear controller is acting:

| | | | |
|---|---|---|---|
| $\Omega_0$ | $u = l_1 x_1 + l_2 x_2$ | $\lvert u_s + v \rvert \leq u_m$ | $\lvert v \rvert \leq v_m$ |
| $\Omega_1^+$ | $u = k_s x_1 + v_m$ | $\lvert u_s + v_m \rvert \leq u_m$ | $v \geq v_m$ |
| $\Omega_1^-$ | $u = k_s x_1 - v_m$ | $\lvert u_s - v_m \rvert \leq u_m$ | $v \leq -v_m$ |
| $\Omega_2^+$ | $u = u_m$ | $u_s + v \geq u_m$ | |
| $\Omega_2^-$ | $u = -u_m$ | $u_s + v \leq -u_m$ | |

In the region $\Omega_0$ the sum of the signal given by the outer loop and the inner loop gives the control strategy to control the position of $x_2$. The controllers active in regions $\Omega_1+$ and $\Omega_1^-$ are designed to give priority to the stabilization of $x_1$ and at the same time to bring the system in the region $\Omega_0$. Let's take in consideration the behavior of the system in $\Omega_1^+$, the results for $\Omega_1^-$ are symmetrical. The control signal that we have in this case is given by:

$$u = k_s x_1 + v_m \tag{2.3}$$

Applying (2.3) to (2.1) gives :

$$\dot{x_1} = -(k_s - 1)x_1 - v_m \tag{2.4}$$

$$\dot{x_2} = k_s x_1 + v_m \tag{2.5}$$

Note that the value of $u$ depends only upon $x_1$, thus the equation (2.4) describing the behavior of $x_1$ is independent from (2.5). The system represented by (2.4) has an equilibrium point $x_1^e$ which is the one that gives $\dot{x_1} = 0$, hence

$$x_1^e = -\frac{v_m}{k_s - 1} \tag{2.6}$$

The equation (2.4) can then be written as:

$$\dot{x_1} = (k_s - 1)(x_1 - x_1^e) \tag{2.7}$$

Since we choose $k_s > 1$ the equation (2.7) represent an asymptotically stable system that converge toward the point $x_1^e$. It is obvious that if we have $|x_1^e| > u_m$ the controller (2.3) will probably bring the system towards instability. Hence when designing the hybrid strategy it must payed attention that the following condition is respected:

$$\frac{v_m}{u_m} \leq k_s - 1 \tag{2.8}$$

It also possible to obtain (2.8) imposing that $u$ given by (2.3) is within the saturation limit for $x_1 = x_1^e$, in fact

$$|v_m + k_s x_1^e| \leq u_m$$

gives (2.8) when using for $x_1^e$ the expression (2.6).
For $x_1 = x_1^e$ equation (2.5) becomes:

$$\dot{x_2^e} = -\frac{v_m}{k_s - 1} \tag{2.9}$$

In the plot 2.2 are reported the trajectories for a system which has $u_m = 1$. For this system it has been chosen a position controller characterized by $\omega = 0.5$ and $\zeta = 0.9$ that give:

$$L = [\,2.15 \quad 0.25\,]$$

For the stabilizing strategy it has been chosen $k_s = 2$ hence:

$$K_s = [\,2 \quad 0\,]$$

and $v_m$ as been set to 0.5. In the plot are also shown the different regions where the different controllers act.

From the figure is clear how the trajectories are driven from the regions $\Omega_1^+$ and $\Omega_1^-$ into the region $\Omega_0$ following the lines $x_1 = \pm x_1^e$. Once the system is in $\Omega_0$ is brought to the origin by the positioning strategy.Note that $|x_1^e| = 0.5 < u_m$.
More graphics related to the evolution of the system having initial conditions $x_1^0 = 0.9$ and $x_2^0 = 7$ are reported in figure 2.3. In this particolar example the system goes from $\Omega_2^+$ to $\Omega_1^+$ and from here to $\Omega_0$. Note that when $x_1$ reaches $x_1^e = 0.5$ the velocity of $x_2$ is constant and negative as shown by formulae (2.9). It is also possible to see how when $v$ is within the saturation limit the signal control $u$ coincide with the signal $u_c$.
In the next plot is shown an example in which the condition (2.8) is not respected. The numerical values used are the same as for the precedent example except for $v_m = 0.8$ and $k_s = 1.7$. The strategy is still working for same initial conditions with a low $x_2^0$. When the initial conditions are more far from $\Omega_0$ the strategy bring the system toward the instability.

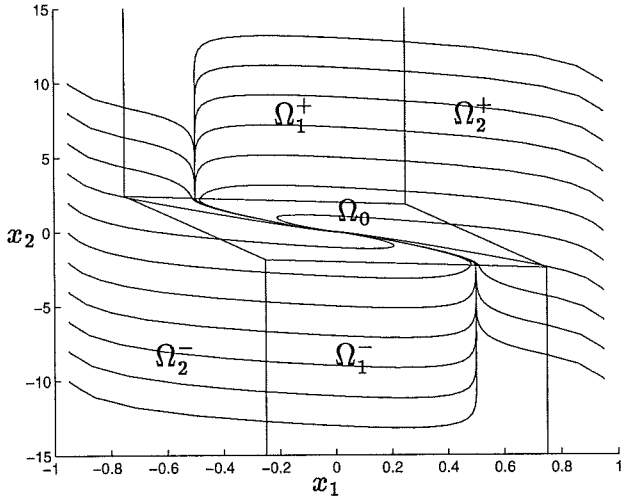


**Figure 2.2** Phase-plots of the system controlled by the hybrid strategy

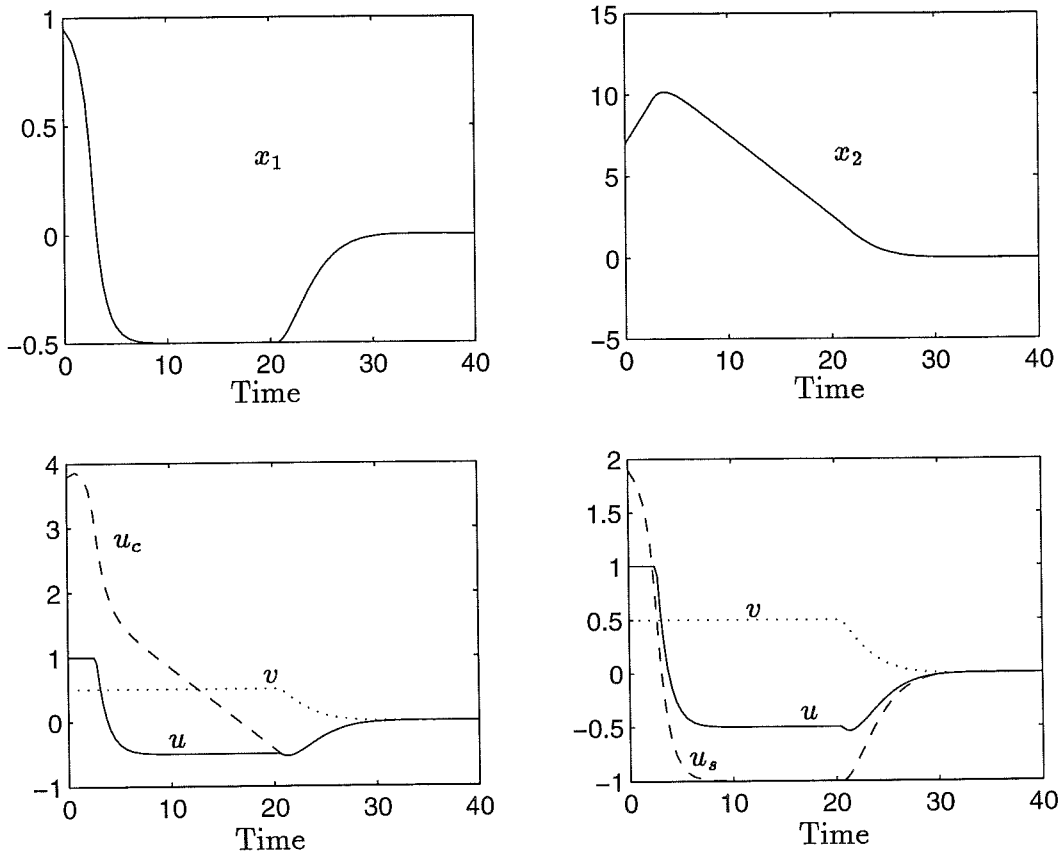


**Figure 2.3** Evolution of the system and control signals for the initial conditions $x_1^0 = 0.95$ and $x_2^0 = 7$

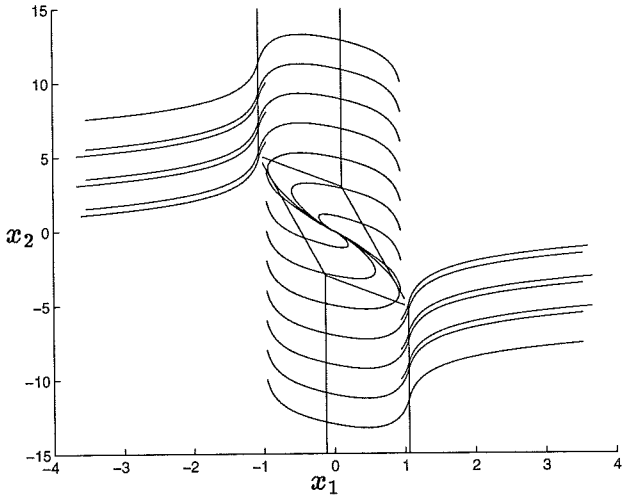


**Figure 2.4** Phase-plots of an unstable example

# 3. Stabilization and Control of an Inverted Pendulum

A characteristic features of the flight control problems discussed in Chapter 1 is to do manual control of an unstable process with actuator limitations. A key difficulty with such a system is that the feedback loop is broken when the actuator saturates. The system will then diverge because of the instability. For such systems it is always possible to find a disturbance which drives the system unstable. It may also be possible to drive the system unstable by inappropriate manual control actions.

Since it is difficult to make experiments with aircrafts we will in this chapter discuss a problem with similar features which can be used more readily for experimentation. The system is the classical inverted pendulum which is used in many control laboratories. We will consider the problem of manual control of the pivot of the pendulum while maintaining the pendulum in the upright position. In particular we will investigate if it is possible to find control strategies which are safe in the sense that the pendulum will remain upright in spite of any manual control input. This problem has several similarities to the flight control problem but there are of course also differences. The dynamics is different. In the flight control problem the actuators are rate limited for the inverted pendulum the main limitation is that the acceleration of the pivot is limited.

In this chapter we will first derive a simple mathematical model for the pendulum and we will then discuss the problem of formulating safe control strategies.

## 3.1 Mathematical models

Assume that the mass of the cart is negligible with respect to the mass of the pendulum and that the motion of the pivot is free of friction. With these assumptions the motion of the cart is described by the simple equation

$$\ddot{x} = a$$

where $m$ is the mass of the pendulum, and $x$ is the position of the pivot in the coordinate system of the figure.

To derive the equations of motion of the pendulum we will use a coordinate system fixed to the cart. In this coordinate frame the position of the pendulum is described by the angular deviation $\theta$ of pendulum from the vertical. The angle $\theta$ is positive in the clock-wise direction. Let the moment of inertia with respect to the center of mass be $J$ and let $l$ be the distance from the pivot to the center of mass. To obtain the equation we will calculate the expression of the potential and Kinetic energy of

the pendulum in the frame fixed to the pivot.
The coordinates of the center of mass of the pendulum are

$$x = l \sin\theta$$
$$y = l \cos\theta$$

The potential energy is thus

$$V = mul \sin\theta + mgl \cos\theta$$

To obtain the kinetic energy we need the velocity of the center of mass. This is obtained by differentiating the position with respect to time. We get

$$\dot{x} = l\dot{\theta} \cos\theta$$
$$\dot{y} = -l\dot{\theta} \sin\theta$$

The kinetic energy is

$$T = \frac{1}{2}J\dot{\theta}^2 + \frac{1}{2}m(\dot{x}^2 + \dot{y}^2) = \frac{1}{2}(J + ml^2)\dot{\theta}^2 = \frac{1}{2}J_p\dot{\theta}^2$$

where $J_p$ is the moment of inertia of pendulum with respect to its pivot point. To obtain the equation of motion we form the Lagrangian $L = T - V$. The equation of motion is then given by

$$\frac{d}{dt}\frac{\partial L}{\partial \dot{q}} - \frac{\partial L}{\partial q} = 0$$

We have

$$\frac{\partial L}{\partial \dot{\theta}} = J\dot{\theta}$$

and

$$\frac{\partial L}{\partial \theta} = mgl \sin\theta - mal \cos\theta$$

The equation of motion thus becomes

$$J_p\ddot{\theta} - mgl \sin\theta + mal \cos\theta = 0 \tag{3.1}$$

### Normalization

The model given by Equation (3.1) has five parameters, the moment of inertia $J_p$, the mass $m$, the length $l$, the acceleration of gravity $g$ and the maximum acceleration of the pivot $u_{max}$. Normalized variable are useful way to characterize the properties of a system.
Introducing

$$\omega_0 = \sqrt{\frac{mgl}{J_p}} \qquad\qquad u = \frac{a}{g}$$

Where $\omega_0$ is the natural frequency of small oscillations around the downward position. The equation of motion then becomes.

$$\ddot{\theta} = \omega_0^2(\sin\theta - u cos\theta) \tag{3.2}$$

Without loss in generality we can choose $\omega_0 = 1$. As emphasized in Åström and Furuta (1996), the properties of the system is thus essentially characterized by one parameter, the maximum acceleration of the pivot $u_0 = a_{max}/g$.

### Problem Statement

Summarizing we find that the model can be described by the equations

$$\begin{aligned} \frac{d^2\theta}{dt^2} &= \sin\theta - u\cos\theta \\ \frac{d^2x}{dt^2} &= gu \\ |u| &\leq u_0 \end{aligned}$$

The problem is to find a control strategy that stabilizes the pendulum in the upright right position and admits manual control of the variable $x$.

It is easier to deal with the linearized problem which is described by.

$$\begin{aligned} \frac{d^2\theta}{dt^2} &= \theta - u \\ \frac{d^2x}{dt^2} &= gu \\ |u| &\leq u_0 \end{aligned}$$

A useful way for many applications to represent a linear system is the state space form:

$$\dot{x} = Ax + Bu \tag{3.3}$$

For the linear model of the pendulum the matrices became:

$$x = \begin{bmatrix} \theta \\ \dot{\theta} \end{bmatrix} \qquad A = \begin{bmatrix} 0 & 1 \\ \omega_0^2 & 0 \end{bmatrix} \qquad B = \begin{bmatrix} 0 \\ -\omega_0^2 \end{bmatrix}$$

If a linear strategy is used to control the system (3.3) we have :

$$u = -Kx \tag{3.4}$$

the closed loop system is then described by:

$$\dot{x} = (A - BK)x \tag{3.5}$$

## 3.2 A Hybrid Strategy

A hybrid strategy will be developed to solve the problem. The idea is to find a control strategy which puts high priority on stabilization of the pendulum and admits manual control of the pivot, provided that it does not violate the stabilization of the pendulum. The strategy will be obtained by patching several control laws together in the spirit of heterogeneous control, see .

### The Energy Controller

The pendulum can always be brought to the upright position by energy control. This strategy is given by

$$u = u_0 \text{sign}(\dot{E}\theta \cos\theta) \tag{3.6}$$

where $E$ is the total energy of the pendulum.

$$E = 1 - \cos\theta + \frac{1}{2}(\dot{\theta})^2$$

See Furuta and Åström (1996).

The energy controller is considered as a last resort. It will always bring the pendulum to the upright position, but there will always be initial conditions such that the pendulum swings by the position where it is straight down, i.e. $\theta = \pi$. We will therefore consider the system "out-of-control" whenever the state $\theta = \pi$ is reached.

Next we will develop a stabilizing controller. This controller will keep the pendulum upright, while disregarding the position of the pivot. To obtain this controller we will first determine the region of attraction, i.e. a region where the pendulum can be brought to the upright position without passing the state $\theta = 0$. We will then find a smaller region where there is a linear stabilizing strategy. We will also determine a region of attraction for this linear strategy.

### The Region of Attraction

The region of attraction is defined as the region where the upward position, $\theta = 0$, can be reached without passing through the position $\theta = \pi$. The rand of the region is given by the trajectories where the acceleration of the pivot has the extreme values. This can be determined as follows. Let the extreme value of the control signal be $u_0$. The equation of motion for the pendulum becomes.

$$\frac{d^2\theta}{dt^2} = \sin\theta - u\cos\theta$$

Multiplying this by $d\theta/dt$ and integrating we get

$$\dot{\theta}\ddot{\theta} = \dot{\theta}\sin\theta - u_0\dot{\theta}\cos\theta$$

Hence

$$\frac{1}{2}\dot{\theta}^2 = -\cos\theta - u_0 \sin\theta + K \tag{3.7}$$

where $K$ is a constant. With extreme values of the acceleration it is possible to keep the pendulum at the equilibrium $\theta_0$ where

$$\theta_0 = \arctan u_0$$

Since this equilibrium must be on the boundary of the region of attraction we find that one boundary of the region of attraction is given by

$$\begin{aligned}\frac{1}{2}\dot{\theta}^2 &= -\cos\theta - u_0 \sin\theta + K \\ &= -\frac{\cos\theta\cos\theta_0 + \sin\theta\sin\theta_0}{\cos\theta_0} + K \\ &= -\frac{\cos(\theta-\theta_0) - 1}{\cos\theta}\end{aligned}$$

where the constant $K$ was chosen to give $\dot{\theta} = 0$ for $\theta = \theta_0$. One boundary of the region of attraction for $|\theta| \leq \frac{\pi}{2}$ is thus given by:

$$\dot{\theta} = \pm\sqrt{2\frac{1-\cos(\theta-\theta_0)}{\cos\theta_0}}$$

For $|\theta| \geq \frac{\pi}{2}$ to have the maximum control action the sign of the maximum acceleration must be reversed, the equation of the boundary thus becomes:

$$\dot{\theta} = \pm\sqrt{2\frac{1-\cos(\theta+\theta_0)}{\cos\theta_0}} + K$$

Where $K$ must be calculated imposing the continuity between the curves. In the same way we find that the other boundary which goes through $\theta = -\theta_0$ and $\dot{\theta} = 0$ for $|\theta| \leq \frac{\pi}{2}$ is given by

$$\dot{\theta} = \pm\sqrt{2\frac{1-\cos(\theta+\theta_0)}{\cos\theta_0}}$$

and for $|\theta| \geq \frac{\pi}{2}$

$$\dot{\theta} = \pm\sqrt{2\frac{1-\cos(\theta-\theta_0)}{\cos\theta_0}} + K$$

A plot of the absorbing regions for different values of $v_0$ are shown in Figure 4.1. As expected it is possible to see from the Figure 4.1 that as we increase the value of $v_0$ the region in which is possible to control the pendulum increases.

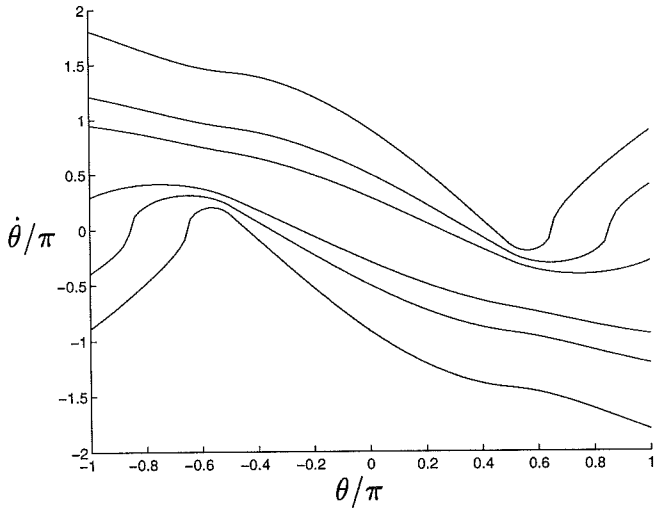


**Figure 3.1** Regions of attraction for $v_0 = 1$, $v_0 = 3$ and $v_0 = 5$

### A Linear Stabilizing Strategy

There are many ways to obtain a linear stabilizing strategy. Since we are also interested in finding the region where it stabilizes the system it is natural to use LQG theory. For linear systems the solution of the Riccati equation automatically gives a Lyapunov function that determines the shape of the region of attraction associated with the optimal controller. The limitations of the control signal determines the size of the region. We can deal with the nonlinear equations as in the previous section by evaluating the derivative of the Lyapunov function along the true nonlinear equation.

Given the linear model

$$\frac{dx}{dt} = Ax + Bu$$

of the pendulum, the LQG theory gives the linear controller that minimize the following cost function:

$$J = \int_0^\infty (x^T Q x + u^T R u) dt$$

Where Q and R are definite-positive symmetric matrices. The optimal controller is given by the state feedback

$$K = R^{-1} B^T S \tag{3.8}$$

where S is the steady-state solution of the Riccati Equation

$$A^T S + SA + Q - SBR^{-1}B^T S = 0 \tag{3.9}$$

The matrix S can be used to form a Lyapunov function

$$V = x^T S x$$

To be a Lyapunov function the function $V(x)$ must have the properties

$$V(0) = 0$$
$$V(x) > 0 for x \neq 0$$
$$\dot{V}(x) \leq 0$$

the first condition is clearly satisfied. The matrix $S$ must be positive definite to satisfy the second condition. The following calculations shows how the third requirement can be fulfilled.

The steady-solution of the Riccati equation S is a positive definite symmetric matrix, this automatically satisfy the first condition. Also the second condition is automatically satisfied, in fact:

$$\dot{V}(x) = \dot{x}^T S x + x^T S \dot{x}$$

using for $\dot{x}$ the expression given by (3.5) we have:

$$\dot{V}(x) = x^t (A^T S + SA - K^T B^T S - SBK) x$$

eliminating $A^T S + SA$ and $K$ using (3.9) and (3.8) the equation becomes:

$$\dot{V}(x) = -x^T (Q + (BS)^T R^{-1T} BS) x \tag{3.10}$$

The matrix $Q$ was assumed to be positive definite and the matrix $(BS)^T R^{-1T} BS$ is positive semidefinite. The matrix $(Q + (BS)^T R^{-1T} BS)$ is definite positive because is obtained as the sum of a positive matrix $Q$ and a positive semidefinite matrix

The existence of a Lyapunov function not only proves that the closed loop system is stable but it also proves that a trajectory starting on the boundary of the set $x|V(x) \leq c$ remains in the set.

The set $x|V(x) \leq c$ is thus a region of attraction for the linear system. We can take the limits on the control signal into account by choosing the parameter $c$ so that the control signal given by $u = -Lx$ is less than the saturation limit. This gives

$$|k_1 \theta + k_2 \dot{\theta}| < u_0 \tag{3.11}$$

The shape of the Lyapunov surfaces $\Omega_c$ depend on the choice of the matrices $Q$ and $R$.

The idea to have a stabilizing region that has a shape similar to the one of the region of attraction leads to the choice of a matrix Q that represent an ellipse with inclined axes. The $Q$ matrix is obtained rotating thediagonal matrix $Q_n$ with the angle $\varphi$. The matrix $Q_n$ representing an ellipse with orthogonal axes that form the angle $\varphi$ with the $x$-axis.

$$Q = N^T Q_n N$$

Where

$$Q_n = \begin{bmatrix} a^2 & 0 \\ 0 & b^2 \end{bmatrix} \qquad N = \begin{bmatrix} \cos(\varphi) & \sin(\varphi) \\ -\sin(\varphi) & \cos(\varphi) \end{bmatrix}$$

We will determine the parameters $a$, $b$ and $\varphi$ so that we obtain an ellipsoid that is well aligned with the region of attraction that was determined in the previous section.

### The Nonlinear Model

There is of course no guarantee that the Lyapunov function found for the linear model will also work for the nonlinear system since we have no guarantee that the conditions (3.10)are satisfied.

To see what happens we introduce

$$V(\theta, \dot{\theta}) = (s_{11}\theta^2 + 2s_{12}\theta\dot{\theta} + s_{22}\dot{\theta}^2)$$

Differentiating respect to time

$$\dot{V}(\theta, \dot{\theta}) = 2 * (s_{11}\theta\dot{\theta} + s_{12}(\dot{\theta}^2 + \theta\ddot{\theta}) + s_{22}\dot{\theta}\ddot{\theta})$$

from (3.2) and (3.4) with $\omega_0 = 1$ we have:

$$\ddot{\theta} = \sin\theta + (k_1\theta + k_2\dot{\theta})\cos\theta$$

Hence

$$\frac{1}{2}\dot{V}(x) = \ddot{\theta}^2(s_{12} - k_2 s_{22}\cos\theta) + \dot{\theta}(s_{11}\theta + s_{22}\sin\theta + k_2 s_{12}\cos\theta + k_1 s_{22}\cos\theta\theta) + (s_{12}\sin\theta\theta + k_1 s_{12}\sin\theta\theta)$$

For $\theta$ close to 0 the right hand side is close to the quadratic form (3.10) obtained for the linearized model.

The constraint give by the saturation of the control signal is

$$k_1\theta + k_2\dot{\theta} < u_0 \tag{3.12}$$

The region in which (3.12) is satisfied shrinks as we decrease R and it increases when $R$ increases. The choice of R is thus a compromise.
The problem now is to find some numerical values for the parameters that characterize the controller that has been described. Several numerical experiments were made for the system characterized by $\omega_0 = 1$ and $v_0 = 1$. This system is characterized by

$$A = \begin{bmatrix} 0 & 1 \\ 1 & 0 \end{bmatrix} \qquad B = \begin{bmatrix} 0 \\ -1 \end{bmatrix}$$

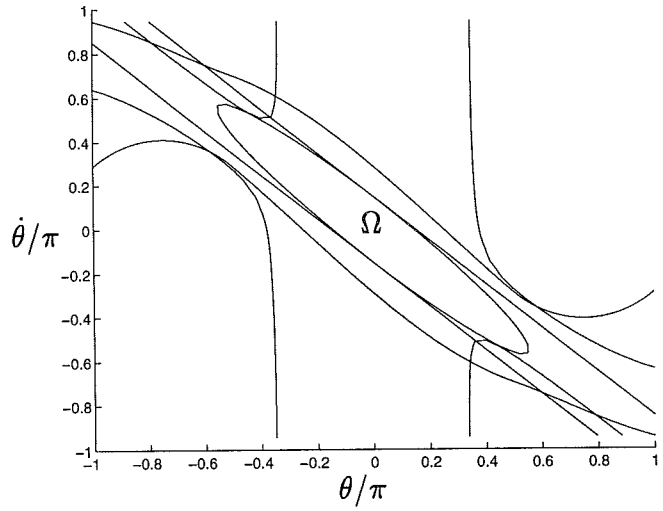


**Figure 3.2** Stabilizing Region $\Omega$ and region of attraction

The values $a^2 = 5$, $b^2 = 1$, $\varphi = 45^0$, and $R = 7$ gave good results. The matrices then have the following values

$$Q = \begin{bmatrix} 3 & 2 \\ 2 & 3 \end{bmatrix} \qquad S = \begin{bmatrix} 16.37 & 15.37 \\ 15.37 & 15.37 \end{bmatrix} \qquad K = [-2.2 \quad -2.2]$$

In Figure 3.2 shows the region of attraction and the following sets

$$V(\theta, \dot{\theta}) = 3 \qquad \dot{V}(\theta, \dot{\theta}) = 0 \qquad k_1\theta + k_2\dot{\theta} = \pm u_0 \tag{3.13}$$

The region $\Omega = \{x | V(x) \leq 3\}$ is the ellipse in the figure. The region where the control signal saturates is represented by the straight lines. And the region where $\dot{V} < 0$ is the dashed region in the figure. The results in the figure were obtained after some experimentation. The figure shows that it is possible to find a region inside the region of attraction where a linear control law can be used.

Some trajectories obtained with the linear control law are shown in Figure 3.3. In this figure we have computed several trajectories of the nonlinear system that originate on the boundary of $\Omega$. This curve verifies the calculations given above which shows that trajectories starting on the boundary remain in the region.

## 3.3 Controlling the position of the Pivot

The strategies discussed until now stabilize the pendulum without considering the the position of the pivot. We will now show how to obtain strategies that stabilize the pendulum and the position of the pivot. Such strategies were derived for example in Åström and Furuta (1995) . The control of the position of the pivot will be done only when the pendulum

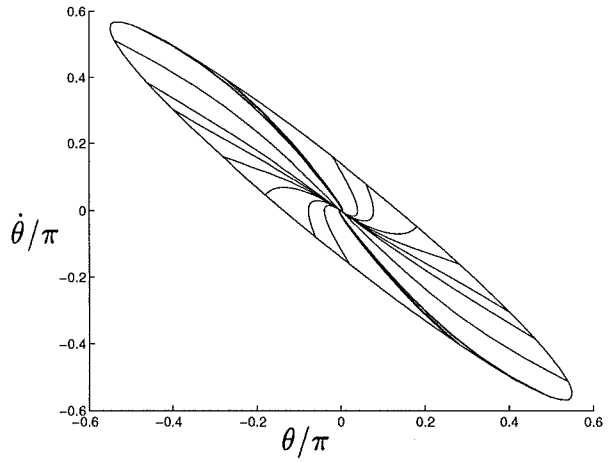


**Figure 3.3** Phase-plots of the evolution of the system for $x_0$ on the boundary of $\Omega$

is in a region smaller than the region of attraction. In this region the angle of the pendulum will be close to the origin. Therefore it makes sense to find a strategy for the linearized model and apply it to the non linear model as it has already been done to find the stabilizing strategy. A linear controller will be used hence:

$$u = l_1\theta + l_2\dot{\theta} + l_3 x + l_4\dot{x}$$

The controlled system in then is described by:

$$\frac{d^2\theta}{dt^2} = \omega_0^2(\theta - l_1\theta + l_2\dot{\theta} + l_3 x + l_4\dot{x})$$
$$\frac{d^2x}{dt^2} = g(l_1\theta + l_2\dot{\theta} + l_3 x + l_4\dot{x})$$

If we apply the Laplace transformation the previous system becomes:

$$(s^2 + \omega_0^2 l_2 s + \omega_0^2 l_1 - \omega_0^2)\Theta(s) = -(\omega_0^2 l_4 s + \omega_0^2 l_3)X(s)$$
$$(gl_2 s + gl_1)\Theta(s) = (s^2 - gl_4 s - gl_3)X(s)$$

Eliminating $\Theta(s)$

$$(s_4 + (\omega_0^2 l_2 - gl_4)s^3 + (\omega_0^2 l_1 - \omega_0^2 - gl_3)s^2 + \omega_0^2 gl_4 s + \omega_0^2 l_3 g)X(s) = 0$$

Assume that we want a closed loop system with the characteristic polynomial:

$$(s^2 + 2\omega_1\zeta_1 + \omega_1^2)(s^2 + 2\omega_2\zeta_2 + \omega_2^2) =$$
$$s^4 + 2(\omega_1\zeta_1 + \omega_2\zeta_2)s^3 + (\omega_1^2 + 4\zeta_1\zeta_2\omega_1\omega_2 + \omega_2^2)s^2 + 2(\zeta_1\omega_1\omega_2^2 + \zeta_2\omega_2\omega_1^2)s + \omega_1^2 + \omega_2^2$$

Identification of coefficients of equal power of s gives the following linear system of equations:

$$\begin{aligned}
\omega_0^2 l_2 - g l_4 &= 2(\zeta_1\omega_1 + \zeta_2\omega_2) \\
-g l_3 + \omega_0^2 l_1 - \omega_0^2 &= 4\zeta_1\zeta_2\omega_1\omega_2 + \omega_1^2 + \omega_2^2 \\
\omega_0^2 l_4 g &= 2(\zeta_1\omega_1\omega_2^2 + \zeta_2\omega_2\omega_1^2) \\
\omega_0^2 l_3 g &= \omega_1^2\omega_2^2
\end{aligned}$$

The solution gives:

$$\begin{aligned}
l_1 &= 1 + \frac{\omega_1^2}{\omega_0^2} + 4\zeta_1\zeta_2\frac{\omega_1\omega_2}{\omega_0^2} + \frac{\omega_2^2}{\omega_0^2} + \frac{\omega_1^2\omega_2^2}{\omega_0^4} \\
l_2 &= \frac{2}{\omega_0}(\zeta_1\frac{\omega_1}{\omega_0} + \zeta_2\frac{\omega_2}{\omega_0} + \zeta_1\frac{\omega_1\omega_2^2}{\omega_0^3} + \zeta_2\frac{\omega_2\omega_1^2}{\omega_0^3}) \\
l_3 &= \frac{1}{g}\frac{\omega_1^2\omega_2^2}{\omega_0^2} \\
l_4 &= \frac{2}{g}(\zeta_1\frac{\omega_1\omega_2^2}{\omega_0^2} + \zeta_2\frac{\omega_2\omega_1^2}{\omega_0^2})
\end{aligned}$$

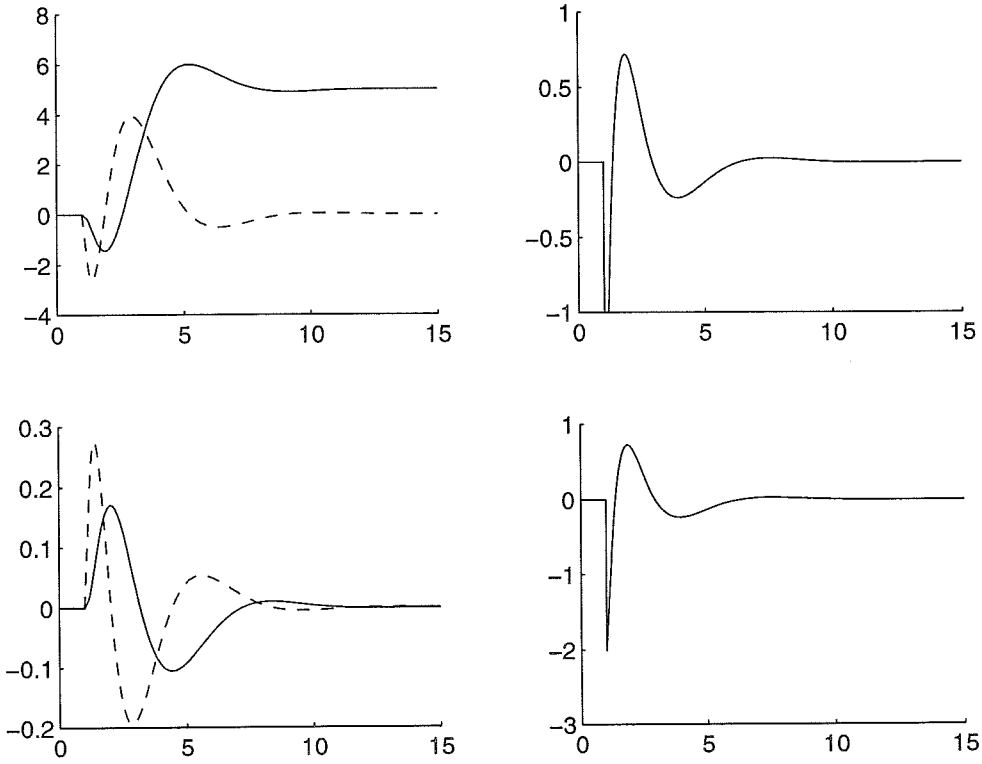


**Figure 3.4** Step response of the pendulum controlled by $L$ with a step $x_s = 5$

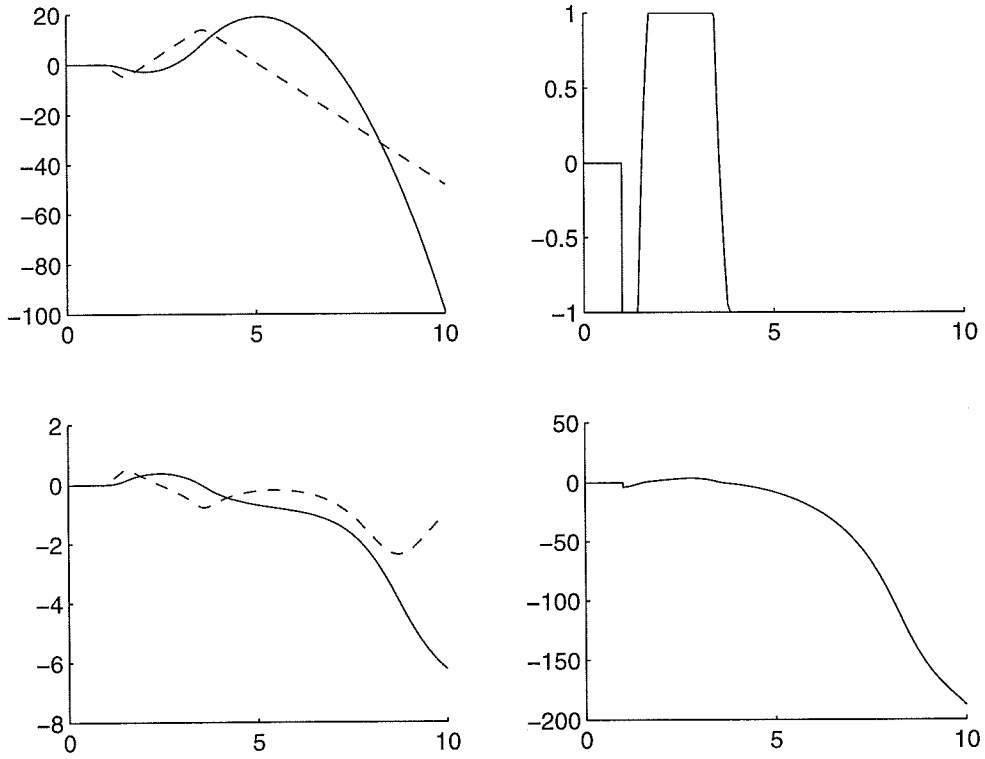


**Figure 3.5** Simulation of the pendulum controlled by $L$ with a step $x_s = 10$ and initial conditions: $x_0 = 0$, $\dot{x}_0 = 0$, $\theta = 0$, and $\dot{\theta}_0 = 0$

Using this strategy is possible to control the position of the pivot if the manual control action is limited. In the next two plots is reported the step response of the system controlled by $L$ for two different values of the input step. For the controller parameters have been chosen:

$$\omega_1 = 2 \qquad \zeta_1 = .9 \qquad \omega_2 = 1 \qquad \zeta_2 = 0.6 \tag{3.14}$$

This values give :

$$L = [14.3 \quad 13.2 \quad .408 \quad 0.857]$$

The initial condition have been set to zero:

$$\theta_0 = 0 \qquad \dot{\theta}_0 = 0 \qquad x_0 = 5 \qquad \dot{x}_0 = 0$$

The simulation in figure 3.3 shows that the strategy works for a step equal to 5.

Figure 3.3 shows an example of how an elevate step input saturates the command signal and bring the system towards instability.

## 3.4 Mixing the strategies

The main task now is to find a strategy that will allow the manual control and at the same time will keep the system stable. To achieve this the

authority of the manual control will be limited following the idea already used in chapter 2 to control a simpler system.
Some consideration on the behavior of the system will lead to modification of the Hybrid scheme that will improve the control strategy for high step input.
The hybrid strategy applied to the pendulum is represented in the figure 3.4 The matrix $Ks$ is obtained with the procedure developed in the sec-

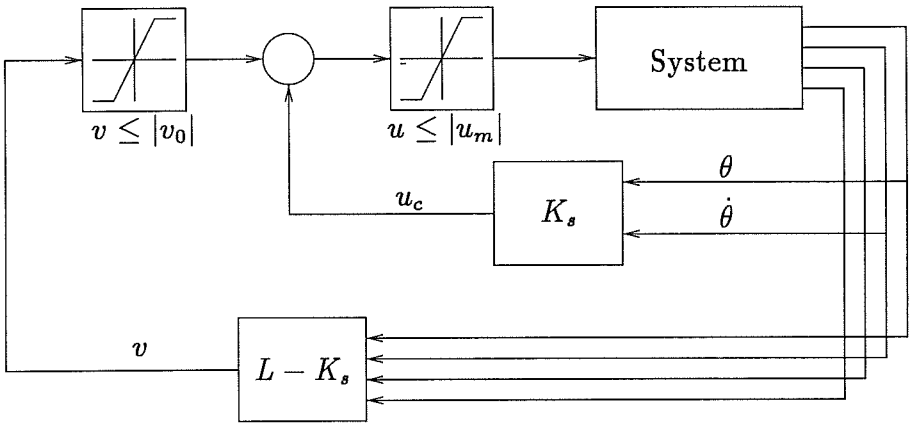


**Figure 3.6** Hybrid strategy applied to the pendulum

tion 'A linear stabilizing strategy' and the matrix $L$ with the procedure described in the section 'Controlling the position of the pivot'.Also the numerical value of $L$ and $K_s$ used in the simulations in this section are the same of the ones used in the example in the others sections.
The authority given to the manual control is represented by the saturation $v_0$.
Due to the passage from two to four dimension and to the non linearity of the problem the analysis of the pendulum controlled by the hybrid strategy is much more complicate than the one of the case examined in chapter 2. It will be in particolar not possible to represent a four dimension region on a paper. Due to the difficulties the analysis will be mainly done commenting the results of some significative simulations. Is anyway possible to do some considerations in this case similar to the ones done for the simpler case.
If both the signal $u$ and $v$ are inside the saturations limits the control signal is given by $L$:

$$\text{if} \quad |v| \leq v_0 \quad \text{and} \quad |u+v| \leq u_0 \quad \Longrightarrow \quad u = u_c = l_1\theta + l_2\dot{\theta} + l_3 x + l_4 \dot{x}$$

When $|v| \geq v_0$ and $|u_s \pm v_0| \leq u_0$ the control signal is given by:

$$u = u_1^{\pm} = \pm v_0 + k_1\theta + k_2\dot{\theta}$$

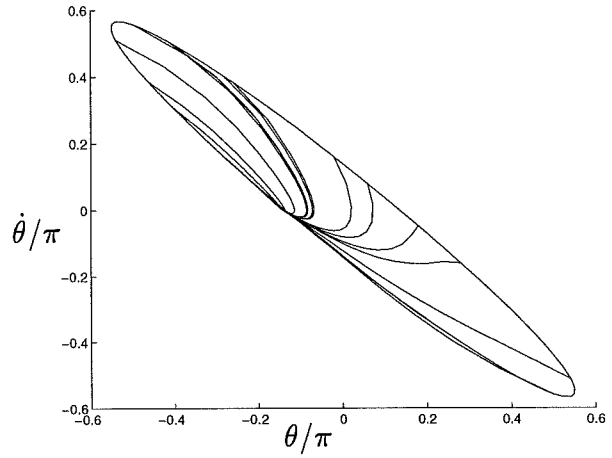


**Figure 3.7** Phase plot of the pendulum controlled by $u_1^+$ with $v_0 = 0.5$

The equation of motion of $\theta$ when the pendulum is controlled only by $u_1^{\pm}$ is then independent from $x$:

$$\ddot{\theta} = \sin\theta - \cos\theta(\pm v_0 + k_1\theta + k_2\dot{\theta})$$

The system represented by the precedent equation has an equilibrium point $\theta_e$ which can be calculated setting $\ddot{\theta}_e = 0$ and $\dot{\theta}_e = 0$:

$$0 = \sin\theta_e - \cos\theta_e(\pm v_0 + k_1\theta_e)$$

Simulations of the pendulum controlled by $u_1^{\pm}$ show that if $\theta_e$ is inside the region of attraction $\Omega$ all the trajectories will converge towards it without going out $\Omega$.
In figure 3.4 are plotted the phase plots for $v_0 = 0.5$ which gives $\theta_e = -0.445$ just on the border of the stabilizing region.
Since the aim of the hybrid strategy is to be able to control the position of the pivot $x$ keeping $(\theta, \dot{\theta})$ inside the stabilizing region $\Omega$, $v_0$ will be chosen to the maximum value that give $\theta_e$ still inside $\Omega$.
Figure 3.4 shows the phase plot obtained when the pendulum is controlled by the hybrid strategy and no command signal is given to $x$. It is possible to see how the trajectory in the plane $(\theta, \dot{\theta})$ don't go out $\Omega$.
If the value of $v_0$ is set to a greater value that 0.5 the trajectories on the plane $(\theta, \dot{\theta})$ will go out the stabilizing region and then out of the region of attraction and hence the system will become unstable. In figure 3.4 is an example of how the system goes out the stabilizing region for $v_0 = 0.7$. The simulations have been stopped to t=300, for grater times some trajectories were going to infinity.

Until now the simulation were obtained with a zero input on $x$, we will now see what happen if we try to control $x$ giving a step command input.
Figure 3.9 reports the phase plot in planes $(\theta, \dot{\theta})$ and $(x, \dot{x})$ of the simulation obtained with a step on $x$ equal to 5 and the initial conditions of

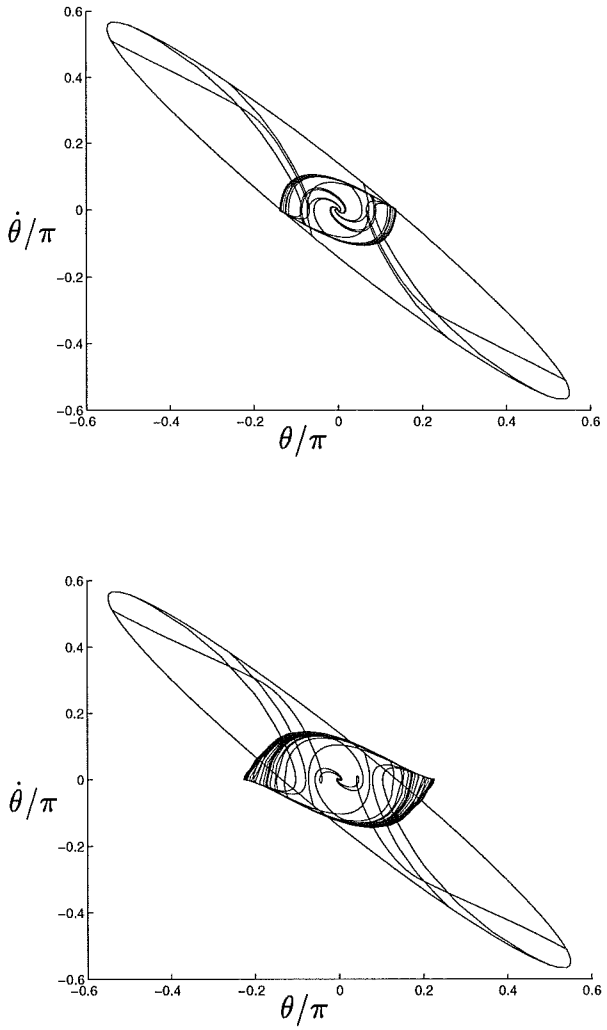


**Figure 3.8** Phase plot obtained with $v = 0.7$ and $x_0 = 0$

$(\theta, \dot{\theta})$ on the border of $\Omega$. It is possible to see that the strategy is able to bring the system to the condition: $x = 5, \dot{x} = 0, \theta = 0, \dot{\theta} = 0$.

Simulations with a step up to $x_i = 1000$ have been done and the strategy was always bringing the system to the desired final condition also if after many oscillations without going out $\Omega$ . A method to eliminate this oscillation will be introduced later.

Since we are mainly interested in the response of the system to command signal on $x$ in the next figures are plotted the state variable and command signals obtained from several step responses in function of time.

To understand how the hybrid strategy works together with the effective control signals $u$ are plotted the signal $v$ and the signal $u_c = Lx$.

Confronting the two figures 3.11 and 3.13 which reports the response to a step of $x_i = 8$ and $x_i = 30$ respectively an important consideration must be done.

If the control signal $u$ switch from $u_c$ to $v_1^{\pm}$ like for the case of $x_i = 30$

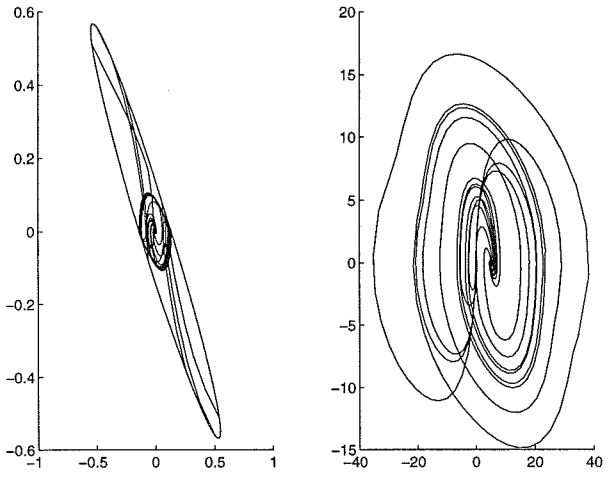


**Figure 3.9** Phase plot obtained with $v = 0.5$ and $x_i = 5$

the pendulum reach the final set after many oscillations. If once the system enter the region in which $u = u_c$ it doesn't go out the final state is reached without any oscillation like in the case of a step input equal to $x_i = 8$.

To avoid this oscillation has been done a modification of the hybrid strategy. Since the oscillations appear for elevate value of the input step it has been introduced a limitation on the error coming from the position of the pivot of the pendulum and going to the controller like in figure 3.12. The value of $x_m$ is the maximum value of $x$ reached in the step response to the maximum step that doesn't cause oscillations. In figure 3.14is reported the responce to a step $x_i = 30$ of the pendulum controlled by the new strategy. Comparing this simulations with the one reported in figure 3.13 is evident the improvement. The set point is reached without oscillations and once the two signals $u_c$ and $u$ became the same they don't diverge anymore. That means that once the system has entered the region where the controller to position the pivot is active doesn't go out anymore.

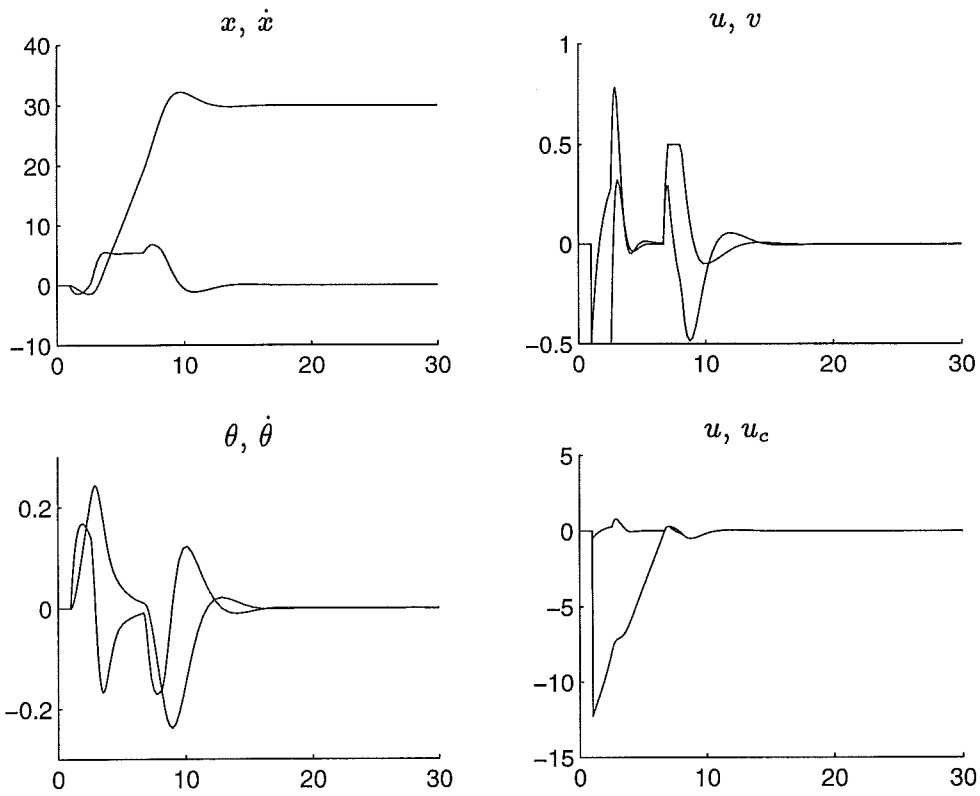


**Figure 3.10** Step response obtained with $v_0 = 0.5$, $x_i = 30$ and initial conditions: $x_0 = 0$, $\dot{x_0} = 0$, $\theta = 0$, and $\dot{\theta_0} = 0$

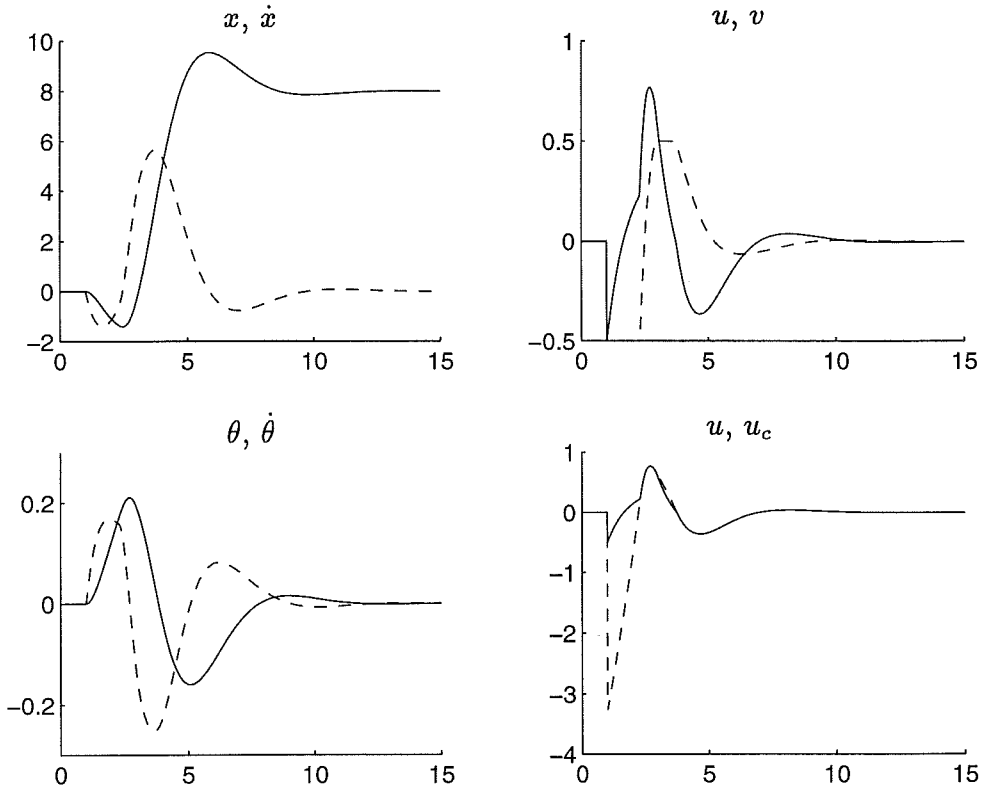


**Figure 3.11** Step response obtained with $v_0 = 0.5$, $x_i = 8$ and initial conditions: $x_0 = 0$, $\dot{x_0} = 0$, $\theta = 0$, and $\dot{\theta_0} = 0$

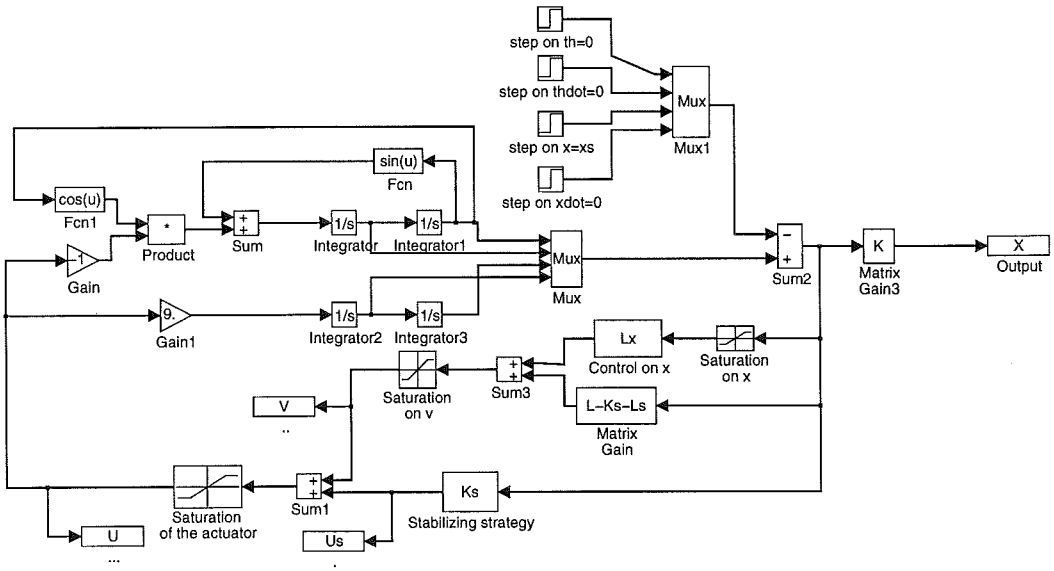


**Figure 3.12** Block-diagram used in simulations

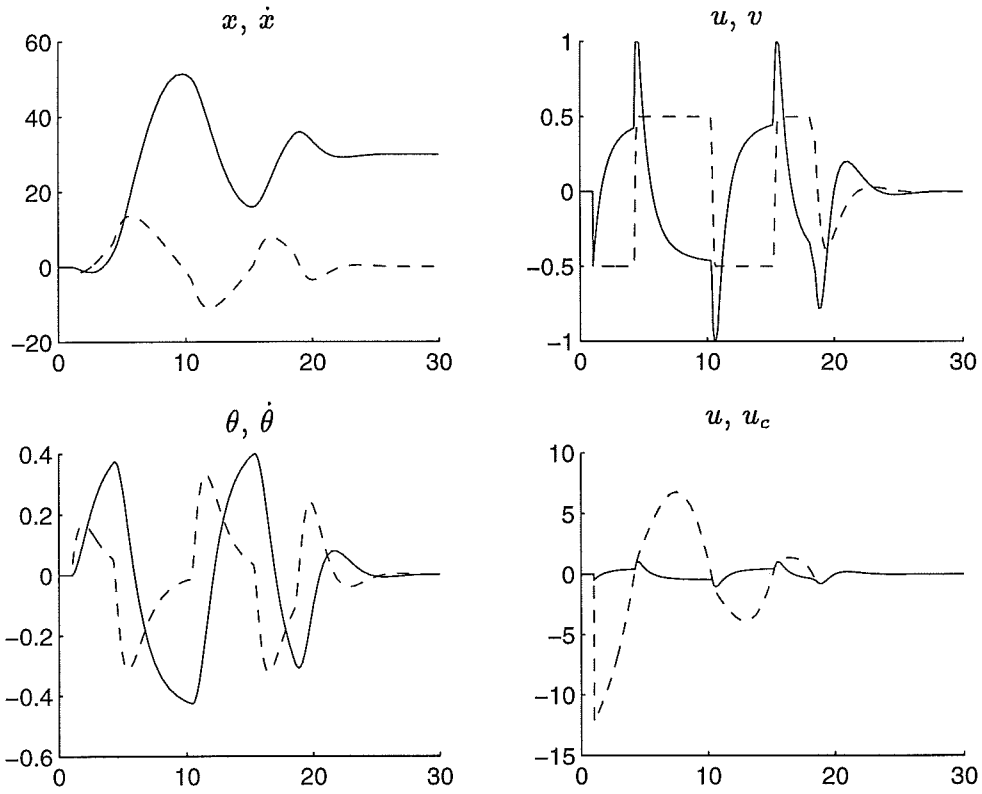


**Figure 3.13** Simulation obtained with $v_0 = 0.5$, $x_s = 30$ and initial conditions: $x_0 = 0$, $\dot{x_0} = 0$, $\theta = 0$, and $\dot{\theta_0} = 0$

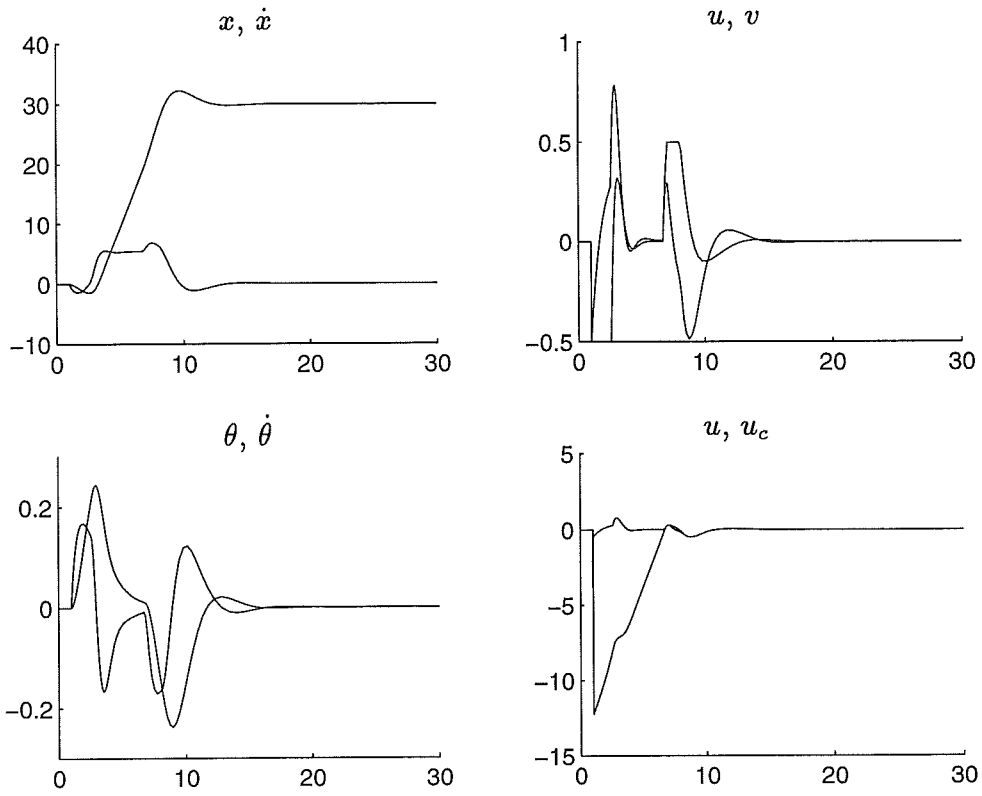


**Figure 3.14** Simulation obtained with $x_m = 11$, $v_0 = 0.5$, $x_s = 30$ and initial conditions: $x_0 = 0$, $\dot{x_0} = 0$, $\theta = 0$, and $\dot{\theta_0} = 0$

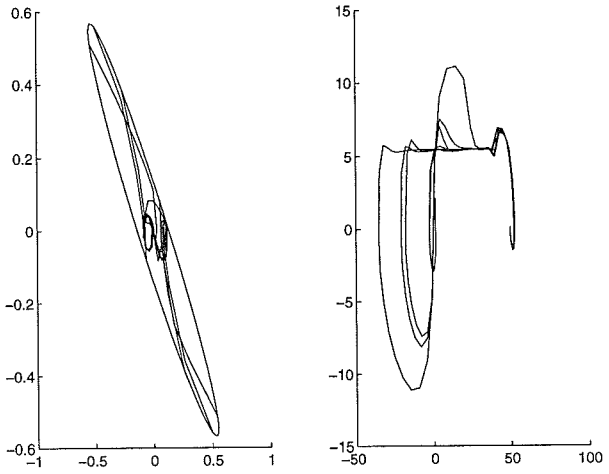

**Figure 3.15** Phase plot obtained with $x_m = 11$, $v = 0.5$ and $x_0 = 30$

# 4. Unstable aircrafts

In this chapter we will deal with the problems related to the control of unstable longitudinal aircrafts. First a brief discussion on the motivations that have lead to the primary importance of automatic control in modern aeronautic is reported. Then a linear model often used to represent the longitudinal dynamic of aircraft will be presented. The factors that contribute to make an aircraft longitudinally unstable will be discussed while introducing the concept of statical longitudinal stability. To complete the chapter an example of how the change of the position of the center of gravity affects the stability is presented.

## 4.1 Longitudinal unstable aircrafts

Flight control system have evolved dramatically over the past few decades. They started as limited authority analogue system, intended to provide a bit of stability augmentation for otherwise well-behaved airframes. They have evolved to full authority digital system, critical to stability and full envelope performance for otherwise unflyable system. There are several example of this phenomena both in military and in civil aeronautics
Traditionally, transport airplanes have been designed to have a certain level of inherent longitudinal stability. This and other control requirements dictate the size of the horizontal tail and restrict the permissible aftmost location of the center of gravity (c.g.). The efficiency of this airplanes can be improved by decreasing the horizontal tail size and moving the c.g. aft. The corresponding reductions in weight and trim drag from the decreased tail size and trim load on the tail can yield a significant reduction in fuel consumption . However this airplanes will have unsatisfactory longitudinal stability and control characteristic. Hence a command and stability augmentation control law is required to provide satisfactionary airplane stability and control characteristic. These problems are particularly critical in hight performance aircrafts where efficiency and performance requirements play a central role. This has lead to the realization of highly unstable aircrafts. The role of the control system is in this cases of priority importance.

## 4.2 Linearized longitudinal dynamic model

To completely describe the behavior of a rigid aircraft six simultaneous non-linear equations are needed, three of them describing the longitudinal dynamic and the other three describing the lateral dynamic.
If we assume that the motion of the airplane consists of small deviations about a steady flight condition we can linearize the equations of motion

obtaining six linear equations. It is possible then to separate the solution of the three equations describing the longitudinal dynamics from the solution of the others if we consider the aircraft to be in straight and level unaccelerated flight condition and then to be disturbed from this condition. Making the following assumptions:

$$\begin{aligned} u &= u_0 + \Delta u & u_0 &= U \\ w &= w_0 + \Delta w & w_0 &= 0 \\ \theta &= \theta_0 + \Delta\theta & \theta_0 &= 0 \\ \Delta q &= \dot{\Delta\theta} \end{aligned}$$

we can obtain the following linear system for the longitudinal dynamic of the aircraft in the form of the state space notation:

$$\begin{bmatrix} \dot{\Delta u} \\ \dot{\Delta w} \\ \dot{\Delta q} \\ \dot{\Delta\theta} \end{bmatrix} = \begin{bmatrix} M_u & X_u & 0 & -g \\ Z_u & Z_w & U & 0 \\ M_u + M_{\dot{w}} Z_u & M_w + M_{\dot{w}} Z_w & M_q + M_{\dot{w}} U & 0 \\ 0 & 0 & 1 & 0 \end{bmatrix} \begin{bmatrix} \Delta u \\ \Delta w \\ \Delta q \\ \Delta\theta \end{bmatrix} + \begin{bmatrix} X_\delta \\ Z_\delta \\ M_\delta \\ 0 \end{bmatrix} [\delta_e] \tag{4.1}$$

Where the elements of the matrix are dependent from the stability derivates through the formulas:

$$\begin{aligned} X_u &= \frac{-(C_{Du} + 2C_{D_0})QS}{mU} & X_w &= \frac{-(C_{D\alpha} - C_{L_0})QS}{mU} \\ Z_u &= \frac{-(C_{Lu} + 2C_{D_0})QS}{mU} & Z_w &= \frac{-(C_{L\alpha} - C_{D_0})QS}{mU} \\ M_u &= C_{mu}\frac{QS\bar{c}}{UI_y} & M_w &= C_{m\alpha}\frac{QS\bar{c}}{UI_y} \\ M_q &= C_{mq}\frac{\bar{c}}{2U}\frac{QS\bar{c}}{I_y} & M_{\dot{w}} &= C_{m\dot{\alpha}}\frac{\bar{c}}{2U}\frac{QS\bar{c}}{UI_y} \end{aligned}$$

And for the control surfaces we have:

$$X_\delta = -C_{X\delta e}\frac{QS}{m} \qquad Z_\delta = -C_{Z\delta e}\frac{QS}{m} \qquad M_\delta = -C_{M\delta e}\frac{QS\bar{c}}{mI_y}$$

To represent the system (4.1) we will use the state space notation:

$$\frac{dx}{dt} = Ax + Bu \tag{4.2}$$

where $x$ and $u$ are called the state vector and the control vector respectively. The matrix A will have for a conventional aircraft two couples of complex conjugate eigenvalues with the real part negative. Hence the longitudinal motion of an aircraft is characterized by two oscillatory stable modes. One is lightly damped and has a long period and for this is called long period-mode the other one is heavily damped and has a very short period and is therefore called short-period.

## 4.3 Longitudinal statical stability of aircrafts

The positions of the aerodynamic center and of the center of gravity are the key elements to determine whether an aircraft is longitudinally stable or not. An aircraft is statical stable if a perturbation on the angle of attack creates a pitching moment that rotates the airplane back in the direction that restore the unperturbated initial flight condition. . Since we can express the dependence of the pitching moment from the angle of attack $\alpha$ with

$$\frac{\partial M}{\partial \alpha} = \frac{1}{2}\rho v^2 S C_{m\alpha}$$

the aircraft is statical stable if

$$C_{m\alpha} < 0$$

The expression of $C_{m\alpha}$ is given by:

$$C_{m\alpha} = C_{L\alpha_w}\left(\frac{X_{cg}}{\bar{c}} - \frac{X_{ac}}{\bar{c}}\right) + C_{m\alpha_f} - \eta V_H C_{L\alpha_t}\left(1 - \frac{d\varepsilon}{d\alpha}\right) \tag{4.3}$$

Where the distances from the wing leading edge to the center of gravity and to the aerodynamic center are denoted by $X_{cg}$ and $X_{ac}$ respectively, and $\bar{c}$ is the wing mean aerodynamic chord. As it can be seen from (4.3) if we move backward the center of gravity we will go towards an unstable configuration. The point in which the center of gravity has to be placed to make the airplane neutrally stable it is called neutral point and it can be calculated by setting $C_{m\alpha}$ equal to zero and solving for the center of gravity position:

$$\frac{X_{NP}}{\bar{c}} = \frac{X_{ac}}{\bar{c}} - \frac{C_{m\alpha_f}}{C_{L\alpha_w}} + \eta V_H \frac{C_{L\alpha_f}}{C_{L\alpha_w}}\left(1 - \frac{d\varepsilon}{d\alpha}\right) \tag{4.4}$$

Note that the position of the neutral point depends upon the aerodynamical data of the aircraft, which means that it will be different for different flight conditions. $C_{m\alpha}$ can now be calculated with the formula:

$$C_{m\alpha} = C_{L\alpha_w}\left(\frac{X_{cg}}{\bar{c}} - \frac{X_{NP}}{\bar{c}}\right) \tag{4.5}$$

This formula shows clearly the dependence of the stability from the position of the center of gravity. The position of the neutral point depend on the flight condition. With this formula it is possible to calculate the position of the neutral point for a particolar flight condition knowing only the position of the center of gravity, the mean aerodynamic chord and the two coefficients $C_{m\alpha}$ and $C_{L\alpha_w}$ . This data can be found in the table included at the end of this chapter for four different flight conditions of the F15. Once $X_{NP}/\bar{c}$ is calculated (4.5) gives the value of $C_{m\alpha}$ for a

particolar flight condition as a function of the position of the center of gravity.
Both the center of gravity and the center of pressure changes with the flight conditions. To illustrate this we will consider the pitch dynamics of the F15.

## 4.4 Longitudinal Dynamic of the F-15

In this section we will give an example of how the position of the center of gravity affects the longitudinal stability of an aircraft. Table XX contains the derivates of stability of four different flight conditions of F-15. With this data and the formulae is possible to obtain the matrix A. All the four flight conditions are characterized by two couples of complex eigen-values with the real part positive which means that the F-15 has a stable longitudinal dynamic in the configurations taken in exam.
The next table contains the value of the natural frequencies and of the damping ratios of the eigen-values for the four flight conditions.

| | First | Second | Third | Fourth |
|---|---|---|---|---|
| Short-Period Damping | 0.3797 | 0.4115 | 0.3360 | 0.2367 |
| Short-Period Frequency | 2.2366 | 4.5098 | 3.2638 | 2.0013 |
| Long-Period Damping | 0.1357 | 0.5144 | 0.2718 | 0.1195 |
| Long-Period Frequency | 0.0780 | 0.0473 | 0.0519 | 0.0572 |

If we move the center of gravity backward the short period will became unstable. In the next graphic is plotted the real part of the eigen-values describing the short period in function of the position of the center of gravity.
It is possible to see how the two complex roots became real and how one of them became positive, making the aircraft unstable.

## 4.5 F-15 DATA

The numerical values of the parameters of the F-15 longitudinal dynamics for four flight conditions are listed in the following table.

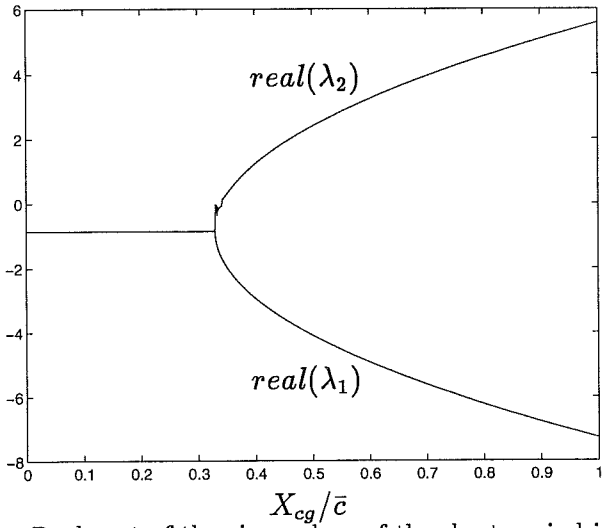


**Figure 4.1** Real part of the eigenvalues of the short period in function of the position of the center of gravity

| | | | | | |
|---|---|---|---|---|---|
| $h$ | (ft) | 20000 | 5000 | 20000 | 40000 |
| $V_t$ | (fpts) | 622.14 | 877.68 | 829.52 | 774.8 |
| $M$ | | 0.6 | 0.8 | 0.8 | 0.8 |
| $WT$ | (lb) | 35900 | 35900 | 35900 | 35900 |
| $q$ | (pfs) | 245.2 | 786.9 | 439.9 | 176.1 |
| $I_y$ | (slut$ft^2$) | 25500 | 25500 | 25500 | 25500 |
| $cg$ | | 26.1 | 26.1 | 26.1 | 26.1 |
| $C_l$ | | 0.24 | 0.075 | 0.135 | 0.335 |
| $C_{l_\alpha}$ | | 4.17 | 4.17 | 4.17 | 4.17 |
| $C_D$ | | 0.05 | 0.05 | 0.05 | 0.05 |
| $C_{D_\alpha}$ | | 0.35 | 0 | 0.21 | 0.764 |
| $C_{m_\alpha}$ | | -0.29 | -0.37 | -0.37 | -0.37 |
| $\frac{c}{2U}C_{m_{\dot{\alpha}}}$ | | 0 | 0 | 0 | 0 |
| $\frac{c}{2U}C_{m_q}$ | | -0.0512 | -0.036 | -0.038 | -0.0412 |

# 5. Hybrid control of longitudinal dynamics

In this chapter is developed an hybrid strategy to control the unstable longitudinal dynamic of an highly manuovrability aircraft. The controllers that will be used in the hybrid strategy have been designed using multi input multi output optimal control techniques.

## 5.1 Model

The model that has been chosen for the simulations is the model of F-15 discussed in chapter one. The control of the longitudinal dynamic is done controlling the positions of the canards and of the elevators. Both the control surfaces are affected by saturations on the value and on their derivate. The dynamic of the control surfaces is described by a first order linear system characterized by a time constant. To make this model representative of a an unstable aircraft the center of gravity has been moved backward to a position that make the short period become unstable as showed in chapter one. The the linearized longitudinal dynamic of the F15 with servo dynamic at 20000 feet and $M = 0.8$ with the position of the center of gravity at $cg = 0.4(MAC)$ is reported in 5.1.

$$\dot{x} = ax + bu \tag{5.1}$$

where:

$$x = \begin{bmatrix} \Delta u \\ \Delta \alpha \\ \Delta q \\ \Delta \theta \\ \Delta \delta_c \\ \Delta \delta_e \end{bmatrix} \quad A = \begin{bmatrix} -0.028 & -0.021 & 0 & -0.038 & 0 & 0 \\ -0.078 & -1.220 & 1.0000 & 0 & -0.717 & -0.143 \\ 0 & 5.364 & -0.972 & 0 & 11.42 & -7.284 \\ 0 & 0 & 1.0000 & 0 & 0 & 0 \\ 0 & 0 & 0 & 0 & -20.00 & 0 \\ 0 & 0 & 0 & 0 & 0 & -20.00 \end{bmatrix}$$

$$u = \begin{bmatrix} \delta_c \\ \delta_e \end{bmatrix} \quad D = \begin{bmatrix} 0 & 0 \\ 0 & 0 \\ 0 & 0 \\ 0 & 0 \\ 20 & 0 \\ 0 & 20 \end{bmatrix}$$

From the analysis of the eigen-values reported in figure 5.1 is clear that the system is unstable. The couple of complex conjugate poles with real part negative describe the phugoid mode. The last two poles describe

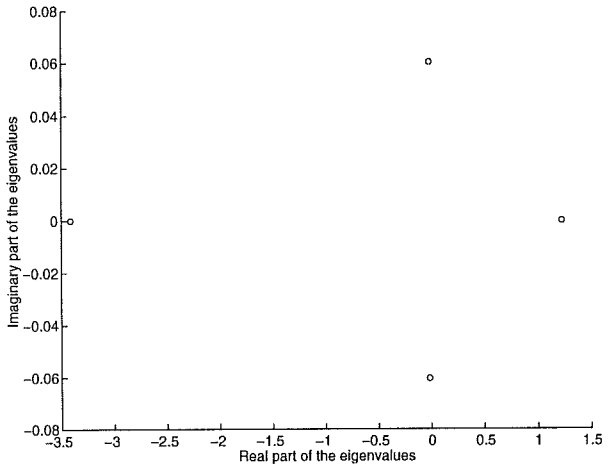


**Figure 5.1** Eigen values of longitudinal dynamic

the short period, and are the degeneration of two complex conjugate poles in two reals, one negative and one positive. Other two real eigenvalues equal to $-20$ representing the dynamic of the actuator are not reported in the figure. The actuators are affected by saturation both on their value and on their derivate:

$$\delta_c \leq 30 \qquad \dot{\delta}_c \leq 200$$
$$\delta_e \leq 30 \qquad \dot{\delta}_e \leq 200$$

## 5.2 Control aims

Due to the presence of the unstable pole it is almost impossible to manually pilotate the aircraft hence is necessary to provide the plane with an artificial stabilizing system.
With the advent of digital control and the availability of multiple surfaces there is an interest in designing control modes for precision flight path control. These modes have the objective of decoupling attitude from flight path control. These non conventional modes offer precise control for certain tasks as well as the possibility of new tactics for the advanced fighters.
The design problem considered here is to decouple the control of the aircraft pitch angle $\theta$ and flight path angle $\gamma = \theta - \alpha$ by the combined use of trailing edge wing flaps and canards. This is equivalent to find a controller that is able to give a precise control of $\theta$ and $\alpha$ .
The controller that will be designed to accomplish these tasks will also stabilize the response of the aircraft to a direct input on the command surfaces.

## 5.3 Control of longitudinal velocity

To obtain a good strategy to control both $\theta$ and $\gamma$ it is necessary the introduction of an automatic system to maintain the longitudinal speed constant using the variation of the throttle. The necessity of velocity control is evident if we think that if we want the aircraft to reach a positive $\gamma$, the aircraft will start to climb decreasing the velocity. To obtain the necessary lift with a lower velocity the angle of attack will increase determinating a compulsory value for the pitch angle.
From (5.1) is possible to calculate the transfer function between the longitudinal velocity and the throttle:

$$\frac{u(s)}{\delta_t} = \frac{s(s+3.4159)(s-1.2230)}{(s+3.4164)(s-1.2259)(s+0.0156+0.0603i)(+0.0156-0.0603i)}$$

As the poles of the short period are practically canceled by the zeros of the transfer function the control of the speed has no effect on the short-period mode.
In the figure 5.2 is reported an automatic velocity control system also called phugoid damping. The time constant for the jet engine is taken at 8 seconds and maybe excessive:however if the system can be made to operate with this lag,its performance would be improved if the actual engine time constant were less. This time lag represents the time required for the trust of the jet to build up after a movement $\delta_t$ of the throttle. Also the dynamic of the throttle is represented by a first order system.
The control action consist on a PID controller and a zero on the whose parameter has been set after several simulations to $K_p = 3, K_i = .5, K_i = .1$. In the feedback loop a zero has been introduced to compensate the time lag caused by the dynamic of the trust. The presence of a derivate on the feed-back explain the low value of $K_i$ in the PID controller. The main part of the derivate action of the controller has been put on the feed-back signal to make the system less sensitive to noise of the reference velocity.
The response to a step of the reference velocity equal to 50 is reported in Figure 5.3.

## 5.4 Design of a controller for the pich and the path angle

If the velocity is kept constant by the automatic control of longitudinal velocity the system describing the rest of the longitudinal dynamic is the fifth order linear system obtained taking out the first row and the first column from (5.1). Now we face the problem of the design of a controller for a multi input multi output system. Given a system in the state space

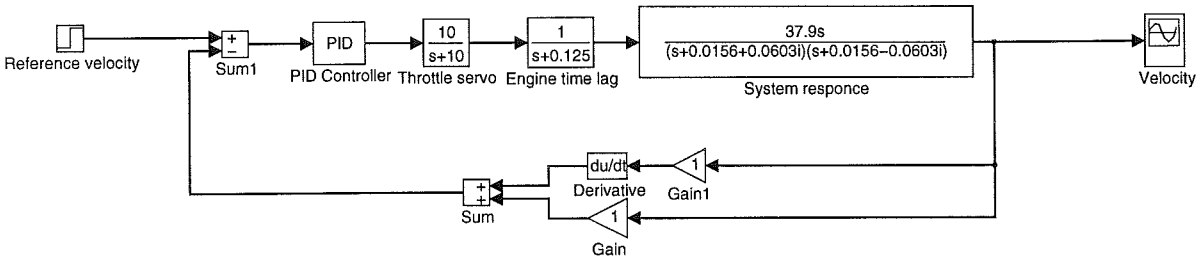


**Figure 5.2** Automatic speed control system

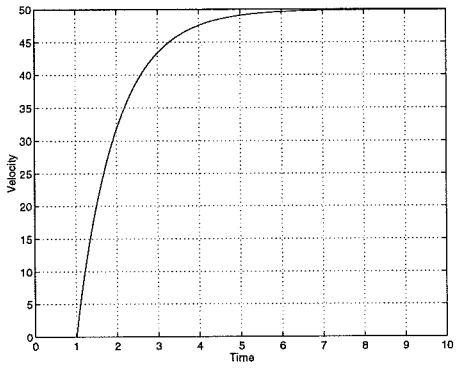


**Figure 5.3** Velocity control with phugoid damphing

form:

$$\dot{x} = Ax + bu$$
$$y = Cx + Du$$

The linear quadratic regulator design for continuous system calculates the optimal feedback gain matrix such that the feedback low $u = -Kx$ minimizes the cost function:

$$J = \int (y^t Q y + u^t R u) dt$$

To have a steady state error equal to zero on $\theta$ and $\alpha$ we must include an integral action in the control loop. Hence the LQG theory has been applied to the system which has as state variables the five initial state variables plus the two integral of the two states that we want to control.

Defining $I_\theta$ and $I_\alpha$ as:

$$I_\alpha = \int \alpha dt \qquad\qquad I_\theta = \int \theta dt$$

The dynamic of the state vectors $x$ is governed by the matrix $A$ :

$$x = \begin{bmatrix} \alpha \\ q \\ \theta \\ \delta_c \\ \delta_e \\ I_\alpha \\ I_\theta \end{bmatrix} \quad A = \begin{bmatrix} -1.2204 & 1.0000 & 0 & -0.7170 & -0.1430 & 0 & 0 \\ 5.3644 & -0.9724 & 0 & 11.4200 & -7.2840 & 0 & 0 \\ 0 & 1.0000 & 0 & 0 & 0 & 0 & 0 \\ 0 & 0 & 0 & -20.0000 & 0 & 0 & 0 \\ 0 & 0 & 0 & 0 & -20.0000 & 0 & 0 \\ 1 & 0 & 0 & 0 & 0 & 0 & 0 \\ 0 & 0 & 1 & 0 & 0 & 0 & 0 \end{bmatrix}$$

The values of the derivate of the actuators is determinate by the difference of the real state of the actuators and state requested by the control action thought the formulas:

$$\dot{\delta}_c = -20(\delta_c - \delta_{cf}) \qquad\qquad \dot{\delta}_e = -20(\delta_e - \delta_{ef})$$

Using these formulas it is possible to have in the output vector $y$ the velocity of the actuators defining the matrix $C$ and $D$ as follows:

$$y = \begin{bmatrix} \alpha \\ \theta \\ q \\ I_\alpha \\ I_\theta \\ \dot{\delta}_c \\ \dot{\delta}_e \end{bmatrix} \quad C = \begin{bmatrix} 1 & 0 & 0 & 0 & 0 & 0 & 0 \\ 0 & 1 & 0 & 0 & 0 & 0 & 0 \\ 0 & 0 & 1 & 0 & 0 & 0 & 0 \\ 0 & 0 & 0 & 0 & 0 & 1 & 0 \\ 0 & 0 & 0 & 0 & 0 & 0 & 1 \\ 0 & 0 & 0 & -20 & 0 & 0 & 0 \\ 0 & 0 & 0 & 0 & -20 & 0 & 0 \end{bmatrix} \quad D = \begin{bmatrix} 0 & 0 \\ 0 & 0 \\ 0 & 0 \\ 0 & 0 \\ 0 & 0 \\ 0 & 0 \\ 20 & 0 \\ 0 & 20 \end{bmatrix}$$

Using the LQR procedure applied to the system above defined is then possible to give weights to all the variables of the problem: actuators and their derivate, pitch and attack angles and their integrals.
From several simulation was clear that while is easy to design a procedure to control $\theta$ leaving unchanged the other variable is much more complicate to control the angle of attack and decouple it from the other variables. This is mainly due to the indifferent behavior that the pitch dynamic shows toward different angle $\theta$ when the velocity is kept cost-ant. While the system is very sensitive to the value of the angle of attack.

The integral action on $\theta$ can cause undesiderable overshoot to correct a steady state error that usually is practically zero, for this the integral action on $\theta$ has been omitted.

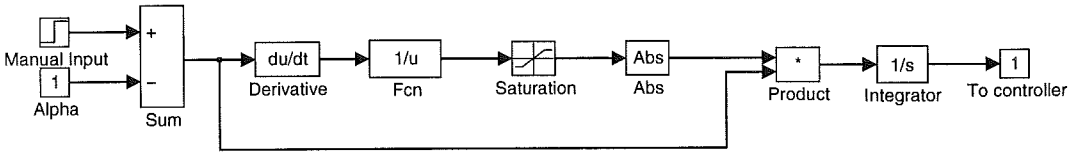


**Figure 5.4** Limitation of integral action on $\alpha$

## 5.5 Limiting the integral action

The fact that $\alpha$ is difficult to control, leaving unchanged at a steady state the other variables, makes the integral action on $\alpha$ essential. On the other hand an integral action can cause overshoots and worsen the response to the commands on the other variable which may request a fast change in the angle of attack.
Hence the integral action on $\alpha$ was limited with a dispositive that will make the integral charge very little when $\alpha$ is far from the set point. To achieve this we use the fact that generally when $\alpha$ is far from the set point $\alpha - \alpha_r$ varies rapidally and hence the derivate on the error on $\alpha$ is big. With this consideration is easy to understand how the scheme block reported in figure 5.4 works. The saturation has been introduced to avoid that when the slope of the error on $\alpha$ is little the signal to the integral becomes infinite.
In figure 5.5 are reported the responses of the aircraft to step manual inputs on $\theta$ and $\gamma$ obtained using the limiter of the integral action and a $Q$ matrix that can be found at the and of the chapter. The first two graphics report the response to the commands $\theta_i = 10$ and $\gamma_i = 10$ which give $\alpha_i = 0$, the set value of $\gamma$ is reached with an overshoot that is caused by the integral action on $\alpha$. The overshoot is decreased by the presence of the limitator of the integral action. The last two graphics report the response to $\theta_i = 10$ and $\gamma_i = 0$ which give $\alpha_i = 10$. In this case the set value of the actuators is different from zero because to keep the aircraft to a different angle of attack we need the actuators to be deflected. From this two examples is possible to see how this controller is able to decouple the control of $\theta$ and $\gamma$.

## 5.6 Stabilizing strategy

The aircraft responses reported on figure 5.5 show a good behavior of the aircraft to limited manual inputs. As the inputs increase the control action saturates the actuators and the system may become unstable. In this paragraph a controller whose only aim is to stabilize the unstable mode of the aircraft will be designed. Making a change of variables thought the

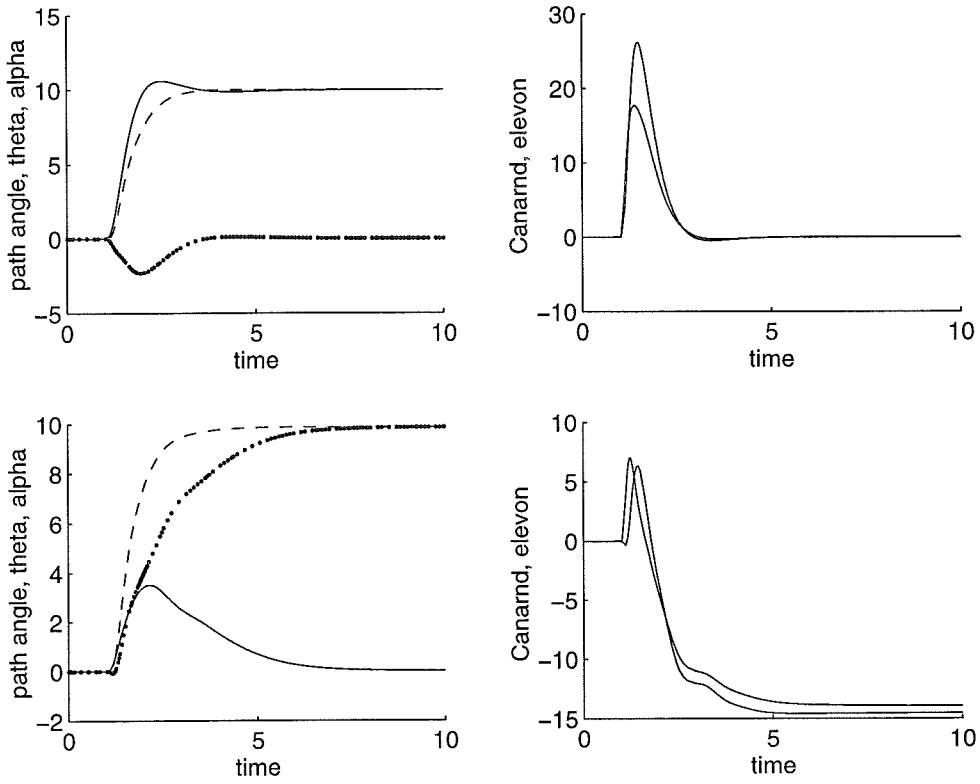


**Figure 5.5** Time response to step inputs: $\theta$ is the dashed line, $\gamma$ is the continue line and $\alpha$ is the dashdot line.

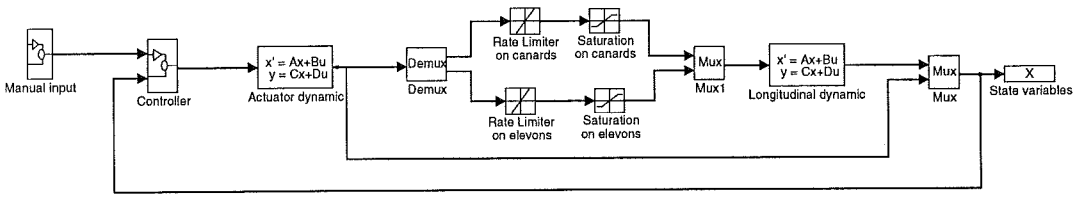


**Figure 5.6** Scheme-block used for simulations

transformation:

$$z = v^{-1}x$$

where the columns of the matrix $v$ are the eigen-vectors of the state

matrix $A$, we get the equivalent diagonal form of the system 5.1.

$$\begin{bmatrix} \dot{z}_1 \\ \dot{z}_2 \\ \dot{z}_3 \\ \dot{z}_4 \\ \dot{z}_5 \end{bmatrix} = \begin{bmatrix} 0 & 0 & 0 & 0 & 0 \\ 0 & 1.2259 & 0 & 0 & 0 \\ 0 & 0 & -3.4159 & 0 & 0 \\ 0 & 0 & 0 & -20.0000 & 0 \\ 0 & 0 & 0 & 0 & -20.0000 \end{bmatrix} \begin{bmatrix} z_1 \\ z_2 \\ z_3 \\ z_4 \\ z_5 \end{bmatrix}$$

With the system in this form is possible to concentrate the control action on the stabilization of the second mode $z_2$ which is the unstable one. This can be done giving practically zeros weight to the control of the other mode in the LQR procedure. The feedback matrix $K_d$ found for the diagonal system must be transformed with the following equation to apply it to the original system:

$$K = K_d * v^{-1}$$

Since the aim of the stabilizing strategy is to stabilize the unstable mode with the limited control action it would useful to have the possibility like in the strategy to control $\theta$ and $\gamma$ to give weights on the actuators and their derivates. This can be achieved applying the LQR procedure to a system which has like output the vector $y$:

$$y^t = [\, z_1 \quad z_2 \quad z_3 \quad \delta_c \quad \delta_e \quad \dot{\delta}_c \quad \dot{\delta}_e \,]$$

which is obtained if we define the matrices $C$ and $D$ as:

$$C = \begin{bmatrix} 1 & 0 & 0 & 0 & 0 \\ 0 & 1 & 0 & 0 & 0 \\ 0 & 0 & 1 & 0 & 0 \\ 0 & 0 & 0 & .84 & 0 \\ 0 & 0 & 0 & 0 & .93 \\ 0 & 0 & 0 & -16 & 0 \\ 0 & 0 & 0 & 0 & -18 \end{bmatrix} \qquad D = \begin{bmatrix} 0 & 0 \\ 0 & 0 \\ 0 & 0 \\ 0 & 0 \\ 0 & 0 \\ 0 & 0 \\ 20 & 0 \\ 0 & 20 \end{bmatrix}$$

Is now possible to design a procedure giving weighs to the actuators their derivates and the unstable mode. Figure 5.7show how the stabilizing strategy is able to bring to zero the unstable mode from an initial condition $z_2 = 100$ without going out the limits of the saturation. Since the the stabilizing strategy was designed giving weights only to the control of $z_2$ and on the actuators and their derivate one of the mode of the system is not brought to zero.

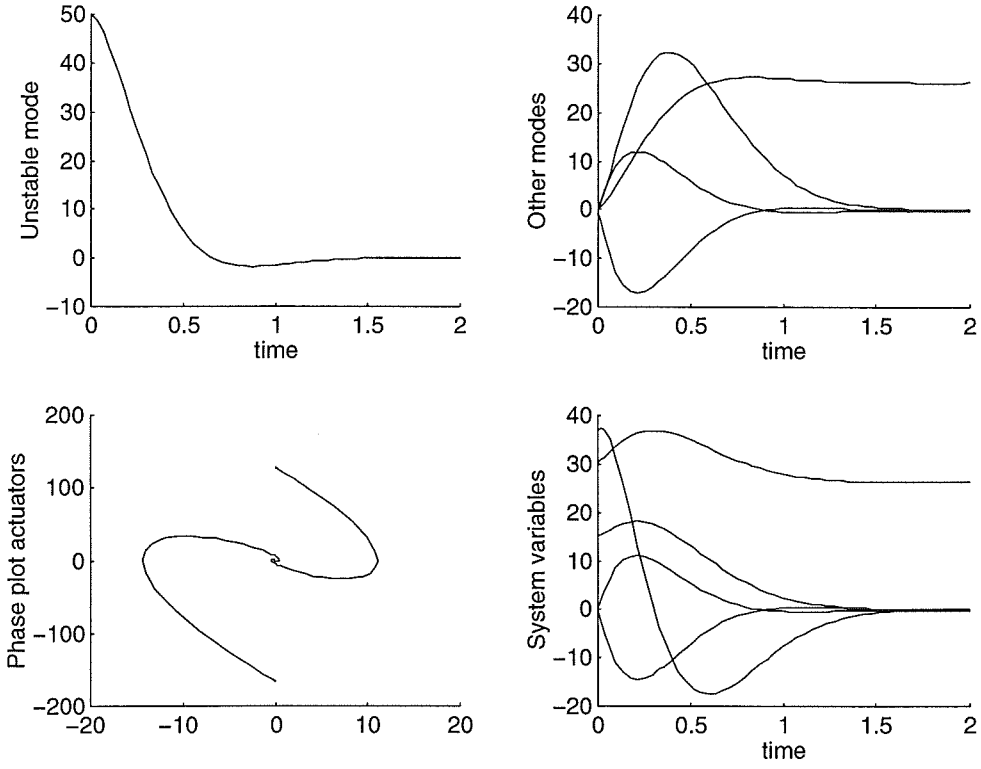


**Figure 5.7** Stabilising strategy

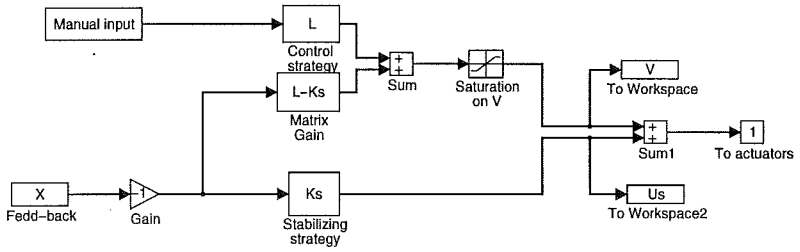


**Figure 5.8** Block-diagram of the hybrid strategy

## 5.7 Hybrid strategy

As it has been done for the othe problems after having designed two control strategies one to stabilize the system and the other one to fulfill the control objectives the next step is to patch them together so that no manual input will drive the system outside the controllability region. The way the two strategies are patched together is reported in the block diagram 5.7. Confronting the next two plots is possible to see the difference between the system controlled by the hybrid strategy and the system controlled by the strategy described in the section **??**. The input

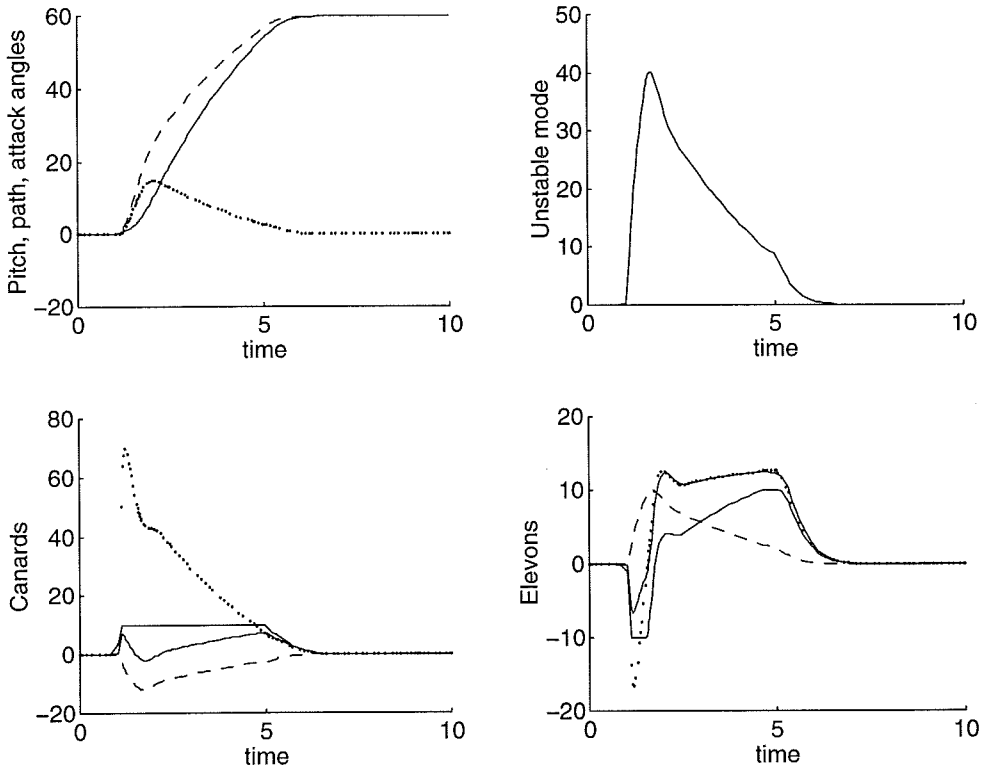


**Figure 5.9** step response of the hybrid strategy

to the system is a very large step on $\theta$. While the system controlled only by $L$ reach the set point with an overshoot and reaching high value of the unstable mode, the system controlled by the hybrid strategy reach the set point without overshoot.

## 5.8 Conclusions

Combining stabilization with manual control is an interesting problem. The attention to this kind of problematic is driven by the increasingly use of automatic control in mission critical applications. The reason for this is the potential benefits and the fact that control engineering is now able to deal with complex systems. Control of high performance aircrafts is a typical example. The design of control laws for unstable systems that make it impossible for the pilot to drive the system unstable while maintaining good handling qualities is a challenging problem. The idea followed in the thesis to solve this problem is the safe mixing of different control strategies. The same idea was applied to different unstable systems. The procedures were developed for the specific problems time by time. It may be interesting to generalize the problem finding some general features that help to deal with a particolar system.
The main attention was devoted to the limitation introduced by the

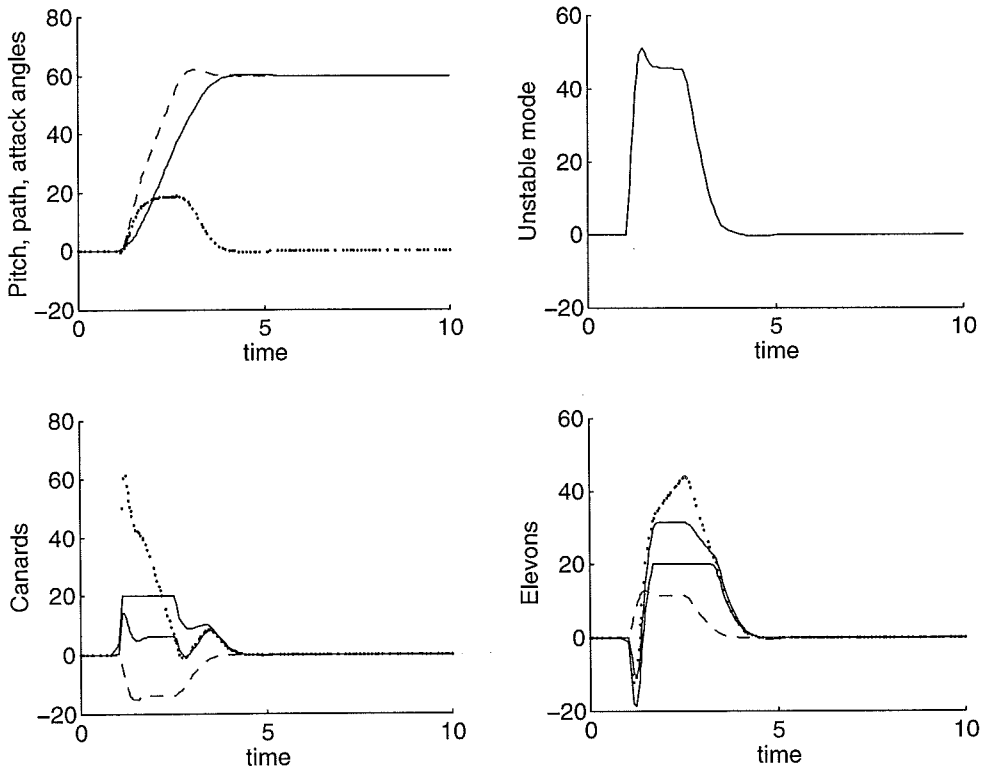


**Figure 5.10** Step response with $v_m = 0$

constraints on the value of the control action. Further investigation can investigate the safe control of system affected by velocity constraints.

# 6. Bibliography


ÅSTRÖM, K. J. and K. FURUTA "Control principles with apllications to pendulums." Technical Report.

ÅSTRÖM, K. J. and B. WITTENMARK (1997): *Computer-Controlled Systems.* Prentice Hall, New Jersey, third edition.

BLAKELOCK, J. H. (1991): *Automatic control of Aircraft and Missiles.* John Wiley & Sons, Inc., second edition.

GLAD, T. (1995): "Stabilizable regions for unstable systems with rate and amplitude bounds on the control." In *IFAC Symposium on Nonlinear Control System Design, NOLCOS'95*, pp. 489–492, Tahoe City, CA.

NELSON, R. C. (1989): *Flight Stability and Automatic Control.* McGraw-Hill.

RUNDQWIST, L. (1996): "Phase compensation of rate limiters in jas 39 gripen." In *AIAA Flight Mechanics Conference*, pp. Paper 96–3368, San Diego, CA.

RUNDQWIST, L. and R. HILLGREN (1996): "Rate limiters with phase compensation." In *Proc. 20th Congress of ICAS*, Sorrento, Italy.

SAFONOV, M. G., A. J. LAMB, and G. L. HARTMAN (1981): "Feedback properites of mulivariable systems: The role and use of the return difference matrix." *IEEE Transaction on Automatic Control*, **AC-26:1**.

STEIN, G. (1990): "Respect the unstable." In *30th IEEE Conference on Decision and Control*, Honolulu, Hawai.

TEEL, A. R. (1992): "Global stabilization and restricted tracking for multiple integrators with bounded controls." *System and Control Letters*, **18:3**, pp. 165–171.

# 7. Appendix

In this appendix two matlab files are reported. They are the matlab-files used in the simulations to plot the regions characterizing the action of the hybrid strategy for the simple problem and for the pendulum.

## 7.1 Simple example

```
%------System
A=[[1 0];[0 0]];
B=[-1 1]';
C=eye(2);
D=[0 0]';
%------Controllers
%--Normal controller
omega=0.5;
damp=0.9;
Le(1,1)=2*omega*damp+omega^2+1;
Le(1,2)=omega^2;
%Le(1,1)=2.4;
%Le(1,2)=0.2;
%-----Closed loop system
Ac=A+B*Le;
%
%--Safe controller
Kes(1,1)=1.7;
Kes(1,2)=0;
%----Parameters of hybrid strategy
%sat1 is the saturation introduced by the hybrid strategy
%sat2 is the real saturation of the sistem
sat1=0.5;
sat2=1;
%------Regions
figure
hold
%Equilibrium point for x1
thetae=-sat1/(Kes(1,1)-1);
thetamin=(-sat2-sat1)/Kes(1,1);
x1min=-1;
x1max=1;
dots=1000;
x2max=15;
x2min=-x2max;
a=0;
```

```
b=0;
c=0;
d=0;
e=0;
f=0;
  x1sat1psat2p=(sat2-sat1)/Kes(1,1);
  x1sat1psat2n=(-sat2-sat1)/Kes(1,1);
  x1sat1nsat2p=(sat2+sat1)/Kes(1,1);
  x1sat1nsat2n=(-sat2+sat1)/Kes(1,1);
for i= 1:dots+1
  x1(i)=x1min+(x1max-x1min)*(i-1)/(dots);
  x2(i)=x2min+(x2max-x2min)*(i-1)/(dots);
  x2sat1p=(sat1-(Le(1,1)-Kes(1,1))*x1(i))/Le(1,2);
  x2sat1n=(-sat1-(Le(1,1)-Kes(1,1))*x1(i))/Le(1,2);
  x2sat2p=(sat2-Le(1,1)*x1(i))/Le(1,2);
  x2sat2n=(-sat2-Le(1,1)*x1(i))/Le(1,2);
  if abs(Le*[x1(i),x2sat1p]') <= sat2
     a=a+1;
     x11(a)=x1(i);
     x21(a)=x2sat1p;
     elseif  abs((Le-Kes)*[x1(i) x2sat2p]') <= sat1
     a=a+1;
     x11(a)=x1(i);
     x21(a)=x2sat2p;
  end
  if abs(Le*[x1(i),x2sat1n]') <= sat2
     b=b+1;
     x12(b)=x1(i);
     x22(b)=x2sat1n;
     elseif  abs((Le-Kes)*[x1(i) x2sat2n]') <= sat1
     b=b+1;
     x12(b)=x1(i);
     x22(b)=x2sat2n;
  end
  if (Le-Kes)*[x1sat1psat2p x2(i)]'>=sat1
    c=c+1;
    x13(c)=x1sat1psat2p;
    x23(c)=x2(i);
  end
  if (Le-Kes)*[x1sat1psat2n x2(i)]'>=sat1
  d=d+1;
  x14(d)=x1sat1psat2n;
  x24(d)=x2(i);
  end
  if (Le-Kes)*[x1sat1nsat2p x2(i)]' <= -sat1
  e=e+1;
  x15(e)=x1sat1nsat2p;
  x25(e)=x2(i);
```

```
  end
  if (Le-Kes)*[x1sat1nsat2n x2(i)]' <=-sat1
  f=f+1;
  x16(f)=x1sat1nsat2n;
  x26(f)=x2(i);
  end
end
 plot(x11,x21)
plot(x12,x22)
plot(x13,x23)
plot(x14,x24)
plot(x15,x25)
plot(x16,x26)
%-----Loop
stop=200;
theta0=0.95;
for x0 = -10:2:10
  [a,b,c]=rk23('example',stop);
  plot(X(:,1),X(:,2))
end
theta0=-0.95;
for x0 = -10:2:10
  [a,b,c]=rk23('example',stop);
plot(X(:,1),X(:,2))
end
theta0=0.95;
for x0 = 2:2:10
  [a,b,c]=rk23('example',stop);
  plot(X(:,1),X(:,2))
end
theta0=-0.95;
for x0 = -10:2:-2
  [a,b,c]=rk23('example',stop);
plot(X(:,1),X(:,2))
end
theta0=0.95;
for x0 = -2:2:2
  [a,b,c]=rk23('example',stop);
  plot(X(:,1),X(:,2))
end
theta0=-0.95;
for x0 = -2:2:2
  [a,b,c]=rk23('example',stop);
plot(X(:,1),X(:,2))
end
```

## 7.2 Inverted pendulum

```
clear x
clear V
clear S
clear K
clear N
clear x1
clear x2
clear dVN
clear A
clear B
figure
hold
%%%%%%%%% PARAMETERS TO CHANGE %%%%%%%%%%%%%%%
%------------System data
% natural frequency of the system
omega=1;
% maximum value of u/g
vo=1;
%----Linear strategy data
% coefficents of the ellipsy
a=sqrt(5);
b=1;
% angle of inclination of the axis of the ellipsy
fi=pi/4;
%---Weight of v in the loss function
R=6.5;
%
%%%%%%%%%%%%%%%%%%%%%%%%%%%%%%%%%%%%%%%%%%%%%%
%-----Linearized system matrices
A=[[0 1];[omega 0]];
B=[0 -omega]';
%
%%%%  Determination of the region of attraction
n=vo;
thetamax=atan(vo);
sup=pi;
inf=-pi;
punti=100;
passo=(sup-inf)/punti;
for i = 26:76
    theta(1,i)=inf+passo*(i-1);
    theta(2,i)=sqrt(abs((cos(thetamax)+n*sin(thetamax)-cos(theta(1,i)
-n*sin(theta(1,i)))*2));
theta(3,i)=-sqrt(abs((cos(-thetamax)-n*sin(-thetamax)-cos(theta(1,i))
+n*sin(theta(1,i)))*2));
```

```
    if theta(1,i) >= thetamax
       theta(2,i)=-theta(2,i);
     end
    if theta(1,i) <= -thetamax
       theta(3,i)=-theta(3,i);
     end
end
for i= 76:101
    theta(1,i)=inf+passo*(i-1);
ra=(cos(pi/2)-n*sin(pi/2)-cos(theta(1,i))+n*sin(theta(1,i)))*2
+theta(2,76)^2;
    theta(2,i)=-sqrt(abs(ra))*sign(ra);
ra= (cos(pi/2)+n*sin(pi/2)-cos(theta(1,i))-n*sin(theta(1,i)))*2
+theta(3,76)^2;
     theta(3,i)=-sqrt(abs(ra))*sign(ra) ;
end

for i=1:25
      theta(1,i)=inf+passo*(i-1);
      theta(2,i)=sqrt(abs((cos(-pi/2)-n*sin(-pi/2)-cos(theta(1,i))
+n*sin(theta(1,i)))*2+theta(2,26)^2));
ra=(cos(-pi/2)+n*sin(-pi/2)-cos(theta(1,i))-n*sin(theta(1,i)))*2
+theta(3,26)^2;
theta(3,i)=sqrt(abs(ra))*sign(ra);
end


%---Plotting the region of attraction--------------------
plot((theta(1,:)/pi),(theta(2,:)/pi))
plot((theta(1,:)/pi),(theta(3,:)/pi))

%%%%%%%%%%
%-----Ellipse matrices
N=[[cos(fi) sin(fi)];[-sin(fi) cos(fi)]];
Q1=[[a 0];[0 b]];
Q=N'*Q1*N;
%
%--Finding the controller with LQR
[K,S,E] = lqr(A,B,Q,R);
%%%%% The next two  loops that calcolate:
%--- the vectors x1, x2 containing the value of
%----the angle and of the angolar
%    velocity in witch are calcolated V and dVN
%----the vectors x1min x1max
%--- the matrices V and dVN in witch are stored the value of
%    the Lyapunov
%    function and the differntial of the lyapunov function.
%
```

```
%--- Limit for the angle of the pendulum
minx1=-pi;
maxx1=pi;
%---Limit for the angolar velocity of the pendulum
minx2=max(theta(2,:));
maxx2=min(theta(3,:));
punti1=50;
um=vo;
for i=1:punti1+1
   x2(i)=minx2+(maxx2-minx2)/punti1*(i-1);
   x1max(i)=um/K(1)-x2(i)*K(2)/K(1);
   x1min(i)=-um/K(1)-x2(i)*K(2)/K(1);
   for j=1:punti1+1
       x1(j)=minx1+(maxx1-minx1)/punti1*(j-1);
   V(i,j)=[x1(j) x2(i)]*S*[x1(j) x2(i)]';
       dVN(i,j)=[x2(i) sin(x1(j))]*S*[x1(j) x2(i)]'
+[x1(j) x2(i)]*S*[x2(i) sin(x1(j))]'
-[x1(j) x2(i)]*K'*B'*S*[x1(j) x2(i)]'*cos(x1(j))
-[x1(j) x2(i)]*S*B*K*[x1(j) x2(i)]'*cos(x1(j));
end
end
%xv is  the point in which a lyapunov surface is tangent to the line
%that delimits the region ni which |v|<vo
xv=vo*[[S(2,2) -S(2,1)];[-S(1,2) S(1,1)]]*K'/(K*[[S(1,1)
-S(1,2)];[-S(2,1) S(2,2)]] *K');
%value of the lyapunov function in x=xv
Vc=xv'*S*xv;
[v d]=eig(S);
% Normalization of the angle and of the angolar velocity.
x1=x1/pi;
x2=x2/pi;
x1max=x1max/pi;
x1min=x1min/pi;
%Plot of V(x)=Vc
contour(x1,x2,V,[0 Vc])
plot(x1max,x2)
plot(x1min,x2)
%Plot of the point in which the derivate of V is zero
contour(x1,x2,dVN,[0 0])
```